Universidade do Minho
Escola de Engenharia

Renato Veloso da Mota

Development of a fast and reliable phage-based method for *Paenibacillus larvae* detection

February 2021

Development of a fast and reliable phage-based method for *Paenibacillus larvae*
Renato Veloso da Mota
UMinho | 2021

Universidade do Minho
Escola de Engenharia

Renato Veloso da Mota

Development of a fast and reliable phage-based method for *Paenibacillus larvae* detection

Master's Dissertation
Master's degree in Biotechnology

Work supervised by
Doctor Ana Oliveira
Doctor Diana Rodrigues

February 2021

Direitos de autor e condições de utilização do trabalho por terceiros

Este é um trabalho académico que pode ser utilizado por terceiros desde que respeitadas as regras e boas práticas internacionalmente aceites, no que concerne aos direitos de autor e direitos conexos.

Assim, o presente trabalho pode ser utilizado nos termos previstos na licença abaixo indicada.

Caso o utilizador necessite de permissão para poder fazer um uso do trabalho em condições não previstas no licenciamento indicado, deverá contactar o autor, através do RepositóriUM da Universidade do Minho.

Acknowledgments

To Doctor Ana Oliveira, for her encouragement and motivation, but especially, for her help and patience during this process.

To Doctor Diana Rodrigues for her genuine disposition to help.

To my colleagues in the Lab, specially Henrique, whom I have relied so many times, and who have always been so supportive. It was a pleasure walking by your side.

To my family. To my parents and brother, for being there during this journey, even with all the difficulties, and for making all this possible from the beginning.

To Patricia, for believing in me when I don't believe in myself. For being the calm in the storm. Everything is so much easier with you.

To Germanio and Carbono for being the greatest source of joy and support that anyone could have.

To whom, in one way or another, contributed to my growth and my future.

Statement of Integrity

I hereby declare having conducted this academic work with integrity. I confirm that I have not used plagiarism or any form of undue use of information or falsification of results along the process leading to its elaboration.

I further declare that I have fully acknowledged the Code of Ethical Conduct of the University of Minho.

Graphical Abstract

I. *P. larvae* spore capture

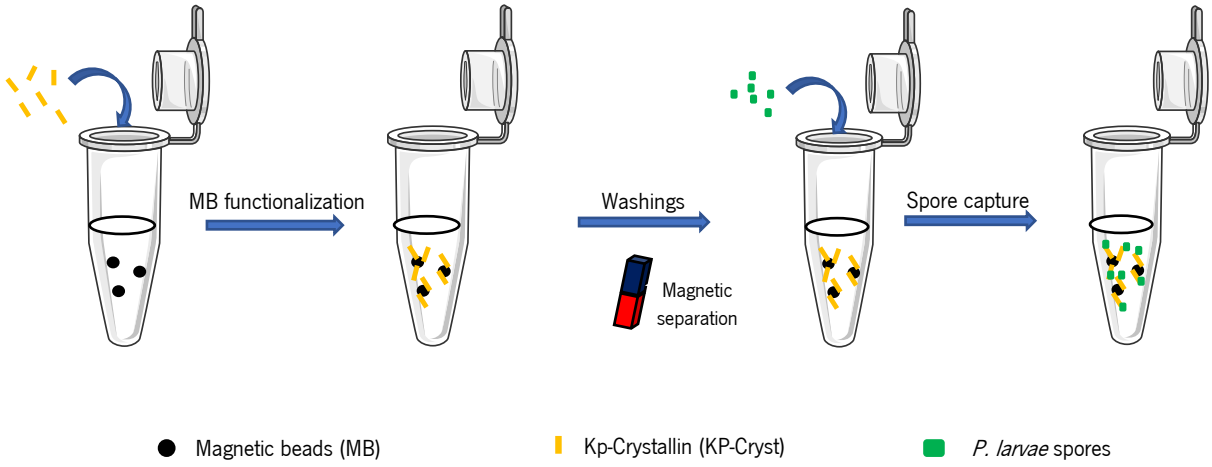

II. *P. larvae* detection

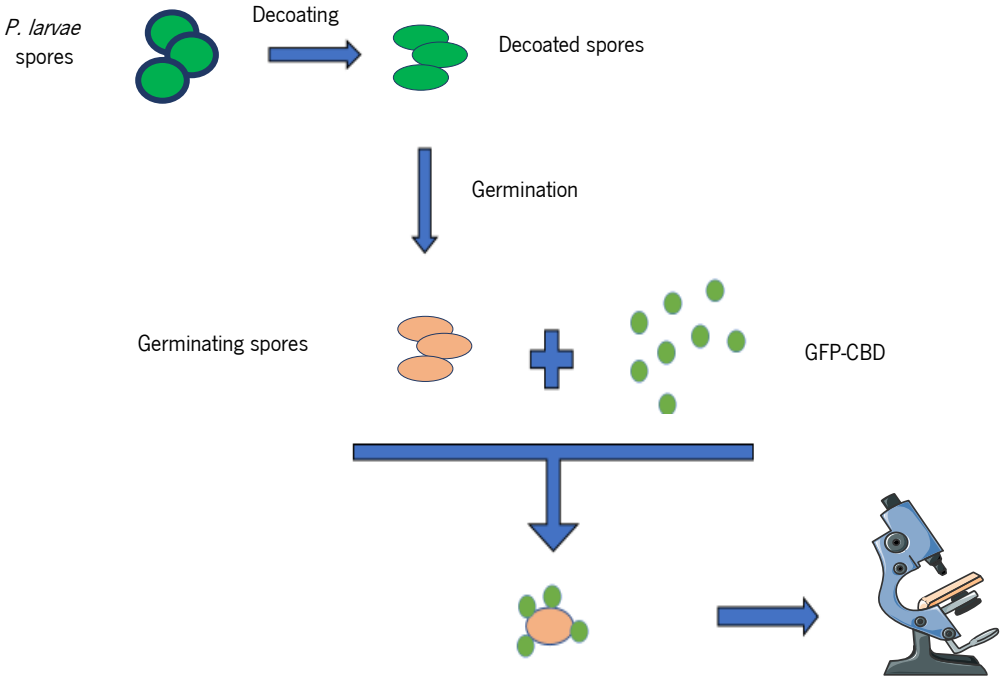

Abstract

Development of a fast and reliable phage-based method for *Paenibacillus larvae* detection

American Foulbrood (AFB) is one of the most important bacterial hive diseases worldwide, affecting honeybee larva. It is caused by the Gram-positive and spore-forming bacterium *Paenibacillus larvae*. Spores are the infectious form of this disease, and its spread in a bee colony often leads to its complete destruction. When the clinical symptoms of AFB appear, the disease can only be controlled by burning the hive. The early detection of *P. larvae* spores will enable the implementation of prophylactic sanitary measures; however, traditional methods are time consuming and often impairs prophylaxis. So far, no effective techniques for spore fast and *on site* detection were developed.

We propose herein a novel method for *P. larvae* spore detection using PlyPl23 CBD. For that, in this work, magnetic beads functionalized with KP-Crystallin (KP-Cryst) – a keratin-like binding protein - will be used to capture and concentrate spores. Nutrient-dependent germination will enable CBD binding and subsequent observation of green-decorated spores by Fluorescence Microscopy.

We monitored spore losses throughout the process and observed that the use of functionalized beads allowed losses similar to those obtained with the currently available method to concentrate and purify spores. In average, 1.2-Log (CFU. mL^{-1}) were lost from a 10^7 CFU.mL^{-1} suspension. A concentration of spores closer to what occurs in the field (10^5 CFU.mL^{-1}) allowed an even lower loss: 0.4-Log (CFU.mL^{-1}).

Besides demonstrating KP-Cryst's ability to bind to keratin-like proteins in the spore coat, it has been shown that PlyPl23 CBD was able to bind to germinating spores, allowing *P. larvae* detection. However, in the presence of homogenized bee mid-hind gut (simulation of real samples) spore capture and CBD-detection were hampered, and no green spores were visualised in the microscopic field from a suspension of 10^7 CFU.mL^{-1} after 4 h of germination. This was possible, yet, after 8 h of germination.

This procedure brings an innovative strategy for *P. larvae* spore capture and subsequent detection in less than 24 h. The use of beads can replace previously used centrifugations steps, showing a high potential for the development of a fast detection KIT for *on-site* application. However, additional optimizations are required to increase the sensitivity of the method in real samples.

Keywords: American Foulbrood; *Paenibacillus larvae* detection; spore; KP-Crystallin; Cell wall binding domain

Resumo

Desenvolvimento de um método rápido e fiável, baseado em fagos, para deteção de *Paenibacillus larvae*

A loque americana (IA) é das mais importantes doenças bacterianas de colmeia a nível mundial, afetando a larva das abelhas. É causada pela bactéria Gram-positiva e formadora de esporos, a *Paenibacillus larvae*. Os esporos são a sua forma infeciosa, onde a sua propagação numa colónia de abelhas leva normalmente à sua total destruição. Quando os sintomas clínicos de IA aparecem, a doença só é controlada através da queima da colmeia. A deteção precoce de *P. larvae* permitirá a implementação de medidas profiláticas sanitárias; mas, os métodos tradicionais são morosos e prejudicam a profilaxia. Até à data, ainda não foram desenvolvidas técnicas eficazes para a sua deteção rápida e no local.

Neste estudo propomos um novo método para a deteção de esporos de *P. larvae* usando PlyPl23 CBD. Para tal, serão utilizadas beads magnéticas funcionalizadas com KP-Cristalina - proteína de ligação tipo queratina - para capturar e concentrar esporos. A germinação dependente de nutrientes permitirá a ligação do CBD e, subsequente observação de esporos verdes através de Microscopia de Fluorescência.

A perda de esporos foi monitorizada ao longo do processo, observando-se que o uso de beads funcionalizadas permitiu perdas idênticas comparativamente ao método atualmente disponível para concentrar e purificar os esporos. Em média, 1.2-Log ($CFU.mL^{-1}$) foram perdidos de uma suspensão 10^7 $CFU.mL^{-1}$. Uma concentração de esporos mais próxima da que ocorre nas abelhas (10^5 $CFU.mL^{-1}$) permitiu uma redução ainda maior: 0.4-Log ($CFU.mL^{-1}$).

Além de demonstrar a capacidade da KP-Cryst se ligar a proteínas semelhantes à queratina na capa do esporo, foi demonstrada a capacidade de ligação do PlyPl23 CBD a esporos germinativos, permitindo a deteção de *P. larvae*. No entanto, na presença de intestino médio de abelha homogeneizado (simulação de amostras reais) a captura de esporos e a deteção por CBD foram prejudicadas, e nenhum esporo verde foi visualizado no campo partindo de uma suspensão de 10^7 $CFU.mL^{-1}$ após 4 h de germinação. Ainda assim, tal foi possível com 8 h de germinação.

Este procedimento representa uma estratégia inovadora para a captura e deteção de esporos de *P. larvae* no prazo de um dia útil. O uso de beads pode substituir etapas de centrifugação, mostrando um elevado potencial para o desenvolvimento de um KIT de deteção rápida para aplicação no local. Contudo, são necessárias otimizações adicionais para aumentar a sensibilidade do método em amostras reais.

Palavras-chave: loque Americana; Deteção de *Paenibacillus larvae;* esporos; KP-Cristalina; Domínio de ligação à parede celular

Table of Contents

List of Figures

List of Tables

List of Abbreviations, Acronyms and Symbols

AFB	American Foulbrood
AB	Antibiotics
B.	*Bacillus*
bp	Base pair
Ca^{2+}-DPA	Dipicolinic acid calcium chelate
CBD	Cell wall binding domain
Cf	KP-Cryst concentration bound to spores or magnetic beads
CFU	Colony-forming unit
Ci	KP-Cryst initial concentration
CO_2	Carbon dioxide
KP-Cryst	Kp-Crystallin
KP-Cryst-Sp	KP-Cryst binding to spores
CTCF	Corrected cell total fluorescence
ddH_2O	Double-distilled water
DL	Deprived from light
DTT	Dithiothreitol
FITC	Fluorescein isothiocyanate
FOM	Fluorescence optical microscopy
g	Gram
g	g-force
h	Hour
HBG	Homogenised bee mid-hind gut
H^+	Hydrogen ion
H27	*P. larvae* PI02-27 strain
IA	Ioque Americana
kDa	Kilodaltons
K^+	Potassium ion
L	Liter
LB	Lysogenic broth
LT_{100}	Time it takes the pathogen to kill 100 % of the infected animals
MB	Magnetic beads
MB-Cap	The quantity of protein that a given volume of MB can capture
MB-KP-Cryst	MB functionalised with KP-Cryst
MB-KP-Cryst-Sp	Spore binding to complex MB-KP-Cryst
MB-KP-Cryst-Sp-CBD	Spore capture and detection system
MB-KP-Cryst : Sp	Ratio between functionalised MB and spores
mg	Milligram
min	Minutes
mL	Milliliter
mM	Millimolar
MPa	Megapascal pressure unit
ms	Millisecond

mV	Millivolt
NaCl	Sodium chloride
NaH_2PO_4	Sodium dihydrogen phosphate
nm	Nanometers
N°	Number
OD	Optical density
P.	*Paenibacillus*
PCR	Polymerase chain reaction
PES	Polyethersulfone
PG	Peptidoglycan
PM	Peritrophic matrix
qPCR	Quantitative PCR
r	Radius
rpm	Rotation per minute
rt	Room temperature
s	Second
SD	Standard deviation
UP	Unbound protein
US	Unbound spores
w/v	Weight per volume
$[Sp]_i$	Spore initial concentration
°C	Degree Celsius
µg	Microgram
µL	Microliter
µM	Micromolar
µm	Micrometers
€	Euro
%	Percentage
>	Superior

Chapter 1. State-of-the-Art

1.1. Background Information

Since ancient times, beekeeping has been a sector of high economic and social standing[1,2]. Honeybees (*Apis mellifera*), besides contributing to a wide variety of ecosystems[3,4] – dependent on the pollination of several native plants - are the most important pollinators for crops that rely on animal pollination for reproduction[5–7]. Furthermore, managed honeybees are responsible for the pollination of about 90 % of all commercial crops[3], worthing worldwide about €175 billion/year[8]. They are, hence, considered the most important pollinators worldwide, and their role in nature is directly linked to food availability and security and, subsequently, to human health[9,10]. In the case of a drastic decrease or even extinction of the honey bee population, humanity would not die, however its diet would be seriously impoverished[3,9].

Notwithstanding the importance of beekeeping, a study exposed the decline in bee population in North America (> 96 %) as well as in its geographical scope (23 – 87 %)[7]. In addition, since 2010, beekeepers have shown unsustainable annual losses of approximately 31 - 46 % of bee colonies[7]. This decrease in pollination bees is associated with several factors, including (a) large-scale conversion of natural landscapes into production-growing fields, resulting in malnutrition and increased exposure of bees to plagues[7]; (b) diseases (bacterial, viral and parasitic) affecting the hives[3]; (c) intensive exposure to pesticides, antibiotics (AB) and agrochemicals used in agriculture and to combat diseases[2,11]. For the former, the continuous application of these products causes a decrease in the longevity of bees as it affects their immune response, learning and olfactory memory, behaviour and forage[7]. Regarding diseases, the most devastating and frequent is bacterial, being known as American Foulbrood (AFB)[12,13].

1.2. American Foulbrood

Honeybees are affected by a wide variety of parasites and pathogens such as viruses, bacteria, and fungi. Some of these pathogens are commensal, while others can kill individual bees or even entire colonies[6].

Paenibacillus larvae is a gram-positive spore-forming bacteria that causes the most destructive bacterial disease ever reported, the American Foulbrood (AFB)[6,14]. This is a highly contagious disease that is lethal to bee larva leading to entire colony destruction[14]. *Apis mellifera*, the world's most important pollinator insect, is the only known host of this bacteria[15]. The AFB was isolated for the first time, in 1989, in Argentina[16]. As it affects bees only in the larval and pupal state it is considered a breeding disease. Nowadays, it is reported worldwide, especially in the United States, Australia, Europe and South

America[13,15]. In Portugal, it occurs in wetter regions and, according to the General Directorate of Food and Veterinary, it is a compulsorily notifiable disease.

The appearance of infected individuals - brown, viscous larvae - arranged in mosaic and with a characteristic odour are the most common clinical symptoms of this disease (**Figure 1**). Viscous threads of larva remains are formed in the alveolus, strongly adhering to its walls and carrying millions of spores, which are the infectious form of these bacteria[17,18].

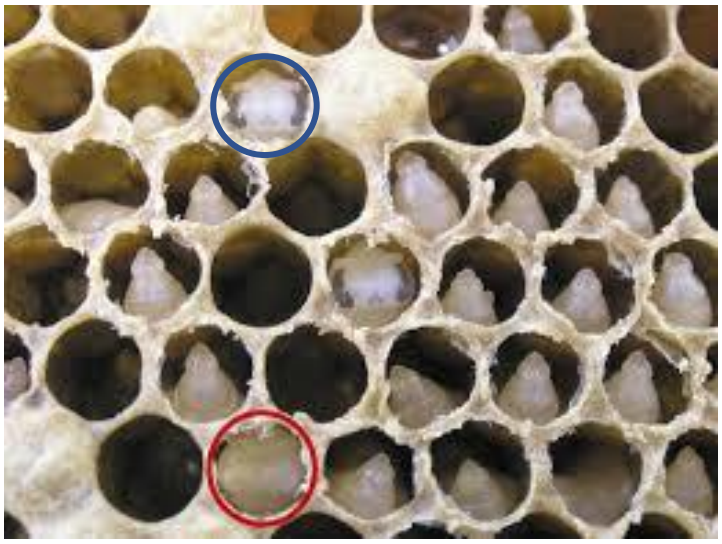

Figure 1. Representation of a healthy larva (dark blue) and an infected larva (red) inside the hive. Adapted from Genersch (2010).

The greatest difficulty in controlling this disease is the easy and rapid spread of spores. The spores are transported by the bees during drifting between hives, by the beekeepers' materials and equipment, and even by contaminated wax, pollen or honey[19–21]. These factors drive the spread of the disease within and between hives.

No effective solution has yet been found for the treatment of this disease. The high resistance of *P. larvae* spores to adverse environmental conditions, such as high temperatures and chemical treatments, as well as their long-term viability make the eradication of spores extremely difficult[21]. Currently, transmission can only be controlled by colony burning, which (a) causes great economic damage to industries and agricultural production depending on pollination; affects the (b) livelihood of beekeepers and (c) affects habitats that rely on these insects for development[19,22]. Moreover, burning the colonies compromises bee biodiversity.

The range of effective antibiotics for AFB (tylosin, lincomycin and oxytetracycline) are poorly metabolised by bees and can remain stable in honey for a long time[23,24]. Consequently, the consumption

of raw honey can be harmful to human health. The selection of AB resistant bacterial strains also represents a well-documented problem to Public Health and to the environment[3,25]. Furthermore, European legislation (CEE n ° 2377/90) forbids the marketing of AB-contaminated honey.

Although easily detectable, clinical AFB symptoms appear late in the hive being only evident after the disease outbreak, when its widespread can no longer be controlled[26]. Hence, for all that has been exposed, early detection of AFB in hives is urgent, and shall enable the implementation of preventive and corrective measures by beekeepers.

1.3. Pathogenesis of AFB

P. larvae is a rod-shaped, facultative anaerobic, peritrichously flagellated and highly motile gram-positive bacteria (0.5 – 0.8 μm wide by 1.5 - 6.0 μm long) that appears either alone or in chains and filaments[27]. Moreover, forms spores under adverse environmental conditions such as lack of nutrients[5]. Spores are the only infectious form of *P. larvae*, and the infection process begins when bee larvae eat food contaminated with those spores provided by honeybees[3]. According to Genersch (2010), the oral uptake of ten spores via contaminated larval food is enough to initiate a fatal infection. Nevertheless, the dose-mortality ratio is influenced by other factors, such as bacterial strain, larval age and genetic constitution[28].

With increasing age, bee larva become less susceptible to infection and two days after hatching they are considered resistant. This age-dependent susceptibility has been attributed to peritrophic matrix (PM) development[9,28,29]. In this context, Yue and colleagues (2008) reported that PM composition and thickness progressively increases with larval age, possibly resulting in an increased ability of the larvae to retain bacteria in the midgut lumen.

The *P. larvae* infection cycle can be divided in five major phases: spore intake, spore germination, vegetative cells proliferation, larvae death and, finally, sporulation (**Figure 2**).

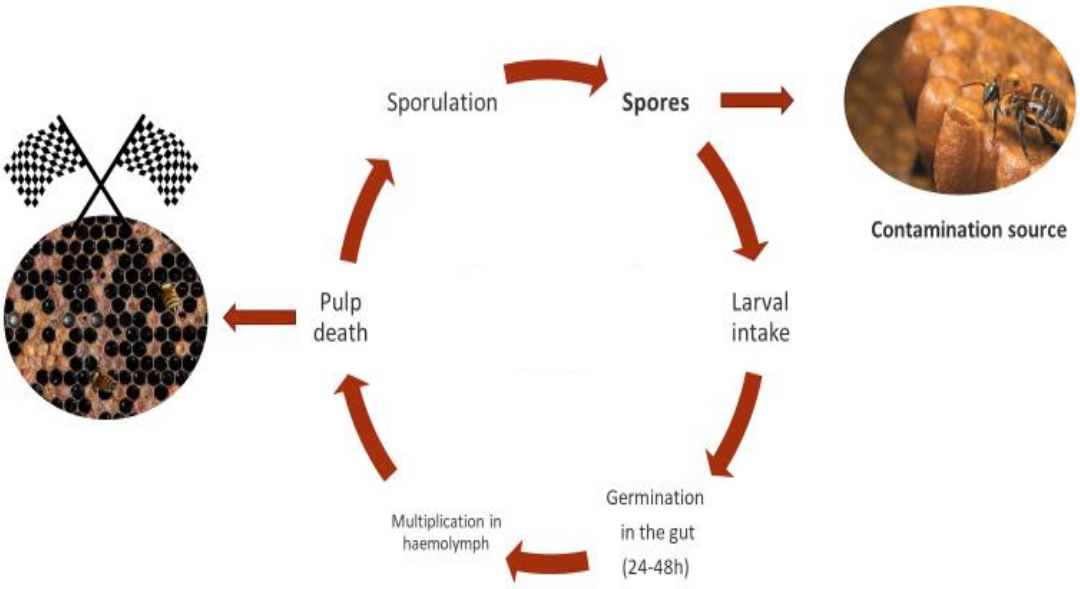

Figure 2. Representation of the infection cycle of *P. larvae* in bee larvae.

Briefly, the infection process starts with the oral uptake of spores by larvae in the first 36 hours (h) after egg hatching[5]. 12 h after ingestion, spores germinate, and the new vegetative bacteria proliferate massively[3,28]. In the next step, *P. larvae* disrupt the intestinal epithelium, with the help of several virulence factors[5] For ERIC I and II genotypes - the two of five genotypes ever reported that caused AFB outbreaks[5,23] - the chitin degrading enzyme PlCBP49 is a key virulence factor, being responsible for the disruption of the PM, which protects the epithelium from pathogen attack[5]. Moreover, while the exclusive *P. larvae* ERIC I toxins PlX1 and PlX2 are relevant for the virulence of the genotype, the SplA surface layer protein expressed exclusively by *P. larvae* ERIC II is essential for its pathogenic strategy, mediating bacterial adhesion to the middle intestinal epithelium[5]. Subsequently, bacteria invade the haemolymph, the infected larva die, and *P. larvae* begins to degrade the larval tissues. The tissue remaining, in the form of a viscous mass containing bacteria, dries out to a scale[9,28]. When the nutrients deplete, the vegetative bacteria begin to sporulate. The dry and ropy mass has billions of spores that spread in and between colonies[2,19,28]. Inside the colony, the spores are transmitted by the adult bees that ingest the remains of the larva, while the bees that steal honey from neighbouring infected hives promote contamination between colonies[3,6,19].

1.4. American Foulbrood control strategies

Some approaches have been proposed and investigated envisaging the control of this disease: (a) treatment with natural antimicrobials such as propolis, essential oils or royal jelly; (b) control by bacteria that inhibit proliferation of *P. larvae*; (c) non-conventional molecules; (d) plant extracts and, more recently, (d) phage therapy.

As far as natural antimicrobial products are concerned, several essential oils were, indeed, considered effective for inhibiting the proliferation of *P. larvae* bacteria[30–32]. Nevertheless, despite promising, this approach still lacks toxicity and *in vivo* studies to support their use in hives[32]. On the other hand, propolis phenolic extracts have proven to be effective and safe therapeutic agents by inhibiting the replication and growth of vegetative cells in the larval gut[33]. Although, additional tests may be required to strengthen these results. Finally, the use of royal jelly to inhibit the growth of *P. larvae* has also been reported in the literature. Mirgorodskaya and colleagues (2009) reported two proteins isolated from royal jelly - royalisin and apalbumin-2a – as having strong antimicrobial activity, *in vitro,* against *P. larvae*[34].

Honeybees are known to harbour a vast microbiome[35]. Therefore, the use of commensal bacteria, which compete and inhibit the proliferation of *P. larvae*, has been suggested for biological control. Lactic acid bacteria found inside the gut of the bee[22], and other bacteria derived from hive by-products such as honey and pollen[36,37], have been shown to be beneficial in controlling this bacterium. Nevertheless, these studies were carried out *in vitro*, requiring then further *in vivo* trials providing data to support the results.

The use of plant extracts with antibacterial properties was another explored strategy. For example, several extracts from the genus Hypericum and the family *Flourensia* showed antimicrobial activity against *P. larvae* and no toxicity to bees[38,39]. More recently, also *Laurus nobilis* extracts[40] and terpenoids[41] revealed to have high activity against this pathogen.

Keeping this same goal, another approach is also being considered. Phage therapy – the use of bacteriophages to kill bacterial cells – holds particular advantages over AB in fighting infections[25,42–44]. Since 2013, when Oliveira and co-authors reported the first *P. larvae* bacteriophage phi_IBB_Pl23, several authors have been reporting effective phages for *P. larvae* control. Some authors performed prophylactic experiments, administering phages prior to *in vivo* infection with spores, with successful results. Nevertheless, its efficiency in treating larva after infection was not consensual[24,45]. On the other hand,

Brady and colleagues (2017) showed that bee larvae sprayed with phages were efficiently protected and rescued from infections caused by *P. larvae*. However, further studies need to be done in order to economize the phages (a lot of waste is generated). More recently, a new podovirus infecting *P. larvae,* API 480*,* widely infecting ERIC I strains but also ERIC II strains, was reported by Ribeiro et al. (2019). This was reported as a phage highly stable when exposed to high glucose concentrations or to larval gastrointestinal conditions[43]. Another important finding reported by Ribeiro and colleagues (2019) was based on a biodistribution experiment that showed that, even though about 10^4 phages have reached the larvae after being uptaken by adult bees, only few maintained an infectious state (i.e. available to control the spread of the disease). They suggested that the inactivation of most phages was due to their exposure to royal jelly, and this way, that they should be protected against hive conditions[44].

Also, phage proteins are being explored. Ply PI23 revealed to be a highly specific endolysin exhibiting high lytic activity against the bacteria[25]. Under pH 7 (occurring in hives), a concentration of 0.2 μM of enzyme was enough to lyse 10^4 CFU.mL^{-1} of *P. larvae* in less than 2 h. Moreover, besides not being inhibited for substances present in bee gut, *in vivo* safety evaluation tests have shown that this protein is not toxic to bee larva[25]. In the same year, PlyPa1A was reported by Leblanc et al. (2015). Using the food, the larvae were simultaneously (a) infected with spores and (b) treated with lysine at a concentration of 16 mg.ml^{-1}. Although mainly active against ERIC I genotypes, the enzyme is not toxic to bee larva and a single dose was able to rescue 75 % of the infected larvae[46].

1.5. Classification of *P. larvae*

Bacteria belonging to the genus *Paenibacillus* have been isolated from a wide variety of habitats, with many being relevant to humans, animals, plants and the environment[47]. Most are found in the soil, often associated with plant roots. Some species produce antimicrobial compounds that can be used in medicine or as pesticides, while others produce enzymes that can be used in the chemical industry[47].

Species of this genus were originally included in the genus *Bacillus* due to the morphological characteristics in common with the species *Bacillus subtilis*, namely its rod-shaped form, its ability to be aerobic or facultative anaerobic and, especially, the ability to produce endospores[47]. Later, a more detailed analysis of phylogenetic relationships between species, relative to the 16S rRNA gene, resulted in the creation of the new genus *Paenibacillus*, which had two species, *P. larvae* and *P. pulvifaciens*[9,48]. However, analyses revealed high similarity at the molecular level between them, and consequently, after several studies and through genotyping and rep-PCR, these species were reclassified into one, *Paenibacillus*

larvae[9,17]. The bacterium presents variable sizes (around 0.5 – 0.8 µm wide by 1.5 – 6.0 µm long) and may occur singly or in chains and filaments, where most strains are mobile[49] (**Figure 3**).

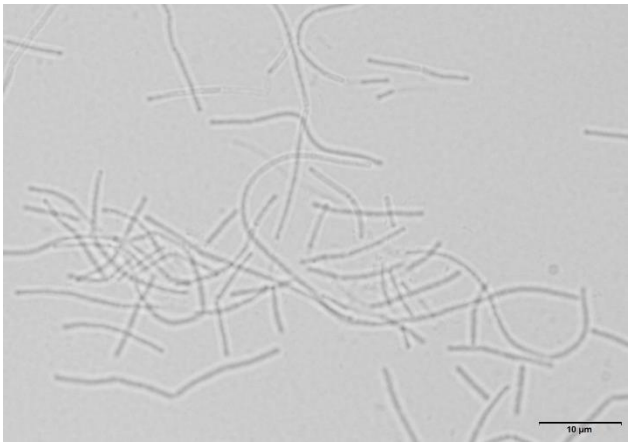

Figure 3. Microscopic image of the H27 strain from the *P. larvae* ERIC I genotype, highlighting its rod-shaped form. Observations were made in bright field. Black bar scale represents 10 µm.

1.5.1. Genotypes and virulence of *P. larvae*

The course and outcome of *P. larvae* infection depends not only on the larval age, as already mentioned, but also on the strain and genotype of the bacteria[28].

Up until now, *P. larvae* comprised four different genotypes (ERIC I - IV) which differ in various phenotypical characteristics, such as metabolism and virulence[9]. However, a few months ago in Spain, Beims and his collaborators (2020) discovered a new genotype, named ERIC V[23]. ERIC I and ERIC II are frequently isolated genotypes from colonies infected by AFB, while few cultures of the other genotypes, ERIC III, ERIC IV, and ERIC V are available, and only in collections.

Table 1. Some characteristics of *P. larvae* genotypes ERIC I, II, III IV and V.

ERIC genotypes	ERIC I	ERIC II	ERIC III	ERIC IV	ERIC V*	References
AFB symptoms	+	+	+	+	+	
LT_{100} (days)	~ 12	~ 7	~ 7/3*	~ 7/3*	~ 3	17
Pigmented colony morphology	-	+	+	-	?	23

*recent characterization by Beims and colleagues (2020)

The most virulent genotypes at the larval level (ERIC II, III, IV and V) requires about 3 to 7 days, while the least virulent genotype at the larval level (ERIC I) needs about 12 days to kill all infected insects[6]. The outbreaks of AFB all over the word are caused by ERIC I and ERIC II[5]. Therefore, the focus of the scientific community falls on them. Following this, the differences in virulence parameters between those are detailed in **Table** 2.

Table 2. Differences between ERIC I and ERIC II genotypes of *P. larvae*, in terms of virulence parameters. Adapted from Genersch et al. (2017)

P. larvae genotypes	Virulence parameters	
	Infected larvae dying before capping (%)	Infected larvae dying in capped cells and developing into ropy mass and foulbrood scales (%)
ERIC I	40 - 60	60 - 40
ERIC II	80 - 95	5 - 20

While most larvae infected with the ERIC II genotype die before cell capping (80 -95 %) being removed by the nurse bees[23,48] - a considerable proportion of ERIC I infected larva die just after metamorphosis (40 to 60 %). In colonies, the ropy mass in the capped cells will dry out to the foulbrood scale, which contains billions of spores, making it easier to spread the disease. Therefore, the more larva die after being capped and without being removed by the nurse bees, the more foulbrood scales will develop, and more spores will circulate in the colony[6]. Hence, the *P. larvae* ERIC I genotype is more virulent at colony level than ERIC II, because colony collapses faster[6,23]. As the ropy mass in capped cells and foulbrood scales are the

clinical symptoms used to diagnose AFB in the field, its symptoms are more easily and rapidly detected in colonies infected with *P. larvae* ERIC I[6]. Thus, false-negative diagnoses are more likely to appear when colonies are infected with *P. larvae* ERIC II due to the hygienic behaviour of nurse bees[48].

Notwithstanding, in both cases colonies will eventually succumb to the disease if left untreated and will be a source of infectious spores for neighbouring colonies. From a diagnostic point of view, the early detection of spores, before any clinical signs appear in the colony, will allow the application of prophylactic sanitary measures by beekeepers, avoiding bee losses[26].

1.5.2. *P. larvae* spores

Some bacteria can survive under adverse environmental conditions, such as starvation, through the formation of stress resistant spores[6]. These structures are capable of withstanding extreme heat, radiation or chemical agents, conditions that would kill any vegetative cell[12,50]. Spores can survive in such a dormant form for decades[51], becoming though the perfect vehicles for infectious diseases[50,52]. When nutrients return to the environment, dormant spores can germinate, reverting to actively growing cells almost immediately.

Dormant spores are composed by many structures, comprising from inside out: the core, an inner membrane, the cortex, an outer membrane, the spore coat, and in some species, the exosporium[53]. Furthermore, structures may vary within the same specie depending on their genetic characteristics[23]. For instance, in *P. larvae*, the ERIC I and II genotypes have a smooth surface, while the other genotypes appear to have ridges[23]. *P. larvae* spores are often found free measuring around1.3 μm long vs 0.6 μm wide[27]. **Figure 4** shows a typical structure of *Paenibacillus larvae* ERIC I spore.

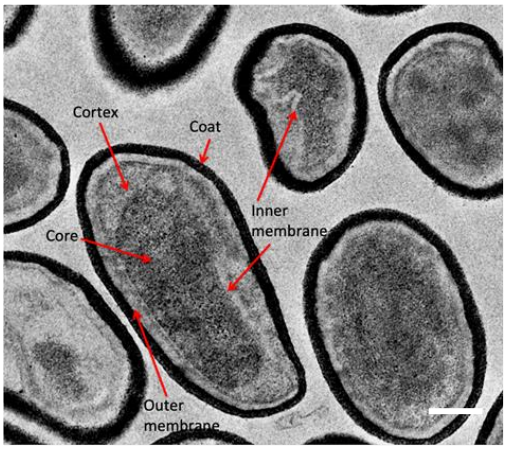

Figure 4. Structure of a *P. larvae* ERIC I spore. (Transmission electron micrographs, 50 000x magnification. Scale bar: 200 nm)

In general, spore core contains all the genetic information necessary for the formation of a functional vegetative cell as well as several small proteins and molecules deposited during spore formation[54]. While some compounds provide resistance during dormancy, others are involved in spore germination and outgrowth[54]. For instance, dipicolinic acid calcium chelate (Ca^{2+}-DPA) is present in very high concentrations in the core and its storage during sporulation contributes to the displacement of water[54]. Surrounding the latter are two different layers of peptidoglycan (PG). The inner layer, highly lipidic, protects the DNA from harmful chemicals, becoming the cell wall of vegetative cells after germination. It is thus known as the germinal cell wall[53,54] and houses the receptors where nutrients will bind to trigger germination[53]. The outer layer is the PG cortex, with high residues of N-acetyl muramic acid and also high enzymatic activity[54]. Additionally, this layer plays a key role in dehydrating the spores, physically restricting the nucleus and preventing its expansion[53,54]. Then, there is a lipid bilayer called outer membrane surrounding the PG cortex that, even not acting as a permeability barrier in the dormant spore, is essential for spore formation[53]. Finally, the spore coat is composed of more than 50 spore-specific proteins, where the function of the most is not known. Despite the practically non-existent information about *P. larvae* spore coat proteins, it is known that the coat of *Bacillus* harbor cortex lytic enzymes, oxidases and others, such as keratin-like proteins. Nevertheless, the coat protects the spore from reactive chemicals and lytic enzymes, being the outermost layer of the *P. larvae* spore[50].

1.5.3. Germination of *P. larvae* spores

Spores are transformed into vegetative bacteria by the germination process, which is a critical step for infection onset in numerous hosts[19]. This process is activated by environmental impulses, which are translated into a series of connected events, resulting in the loss of the properties of dormant spores[52].

In general, germination might be triggered by two routes: (a) nutrient-dependent or (b) nutrient-independent ones. While the first includes low molecular weight compounds – specie and strain specific – such as amino acids, sugars and purine derivates[50], the second one comprises Ca^{2+}-DPA, lysozyme, cationic surfactants, high pressure, among others[50,53].

Nutrient-dependent germination results from the passage of the germinants through the spore's outer layers, which is facilitated by the presence of specific coating proteins[50]. When the environmental conditions are favourable, the sensory mechanisms of the spore surface detect the respective germinants leading to germination[50]. Regarding nutrient-independent pathway, it may be started in 3 distinct ways: high pressures activate (a) the germinating receptors (100-200 MPa); or (b) the release of Ca^{2+}-DPA (500-

600 MPa); while (c) alkylamines activate the release of Ca^{2+}-DPA either directly or indirectly by effects on the internal spore membrane. Consequently, the Ca^{2+}-DPA activates cortex enzymes, like CwlJ, which will cause cortex hydrolysis and, subsequently, result in the formation of a vegetative cell[53]. In addition, it is also known that treatment with lysozyme causes hydrolysis of the cortex, which in some way causes the release of Ca^{2+}-DPA[53].

The nature of the spore germination signals has been widely studied in *Bacillus* and *Clostridia*, but only recently *P. larvae* germination process has beginning to be discovered. Alvarado and colleagues (2013) showed that *P. larvae* spores specifically recognized L-tyrosine and uric acid as germinants. This nutrient-dependent germination can be described as a single integrator logical gate, where multiple germinants must interact individually with their respective receptors, and more than one germinating agent must be present to activate germination[19,52]. In *P. larvae* spores, each receptor recognizes its own germinating agent (uric acid and L-tyrosine). Although the germination mechanism of *P. larvae* is not fully understood, it is known that its genome encodes putative germination receptors similar to those found in *Bacillus* and *Clostridium* species[12], being a general scheme of this process represented in **Figure 5**.

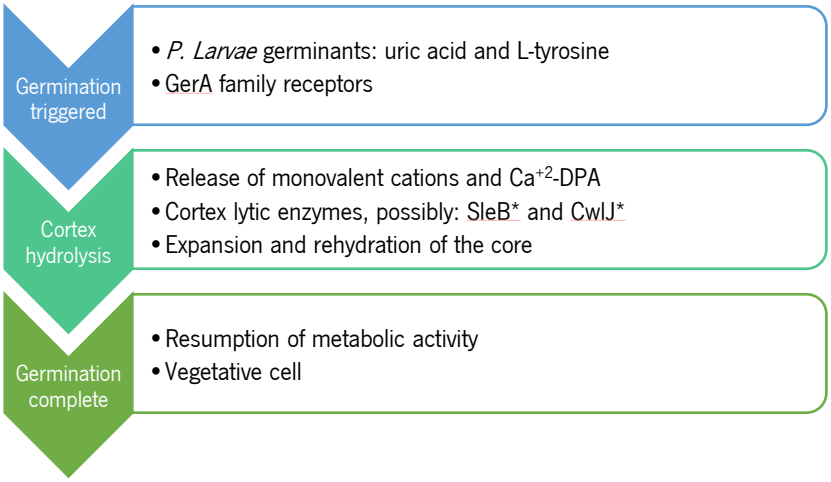

Figure 5. Scheme of *P. larvae* spore's germination. *Cortex lytic enzymes presumably involved in *P.larvae* spore's germination process.

Briefly, when the germinants, uric acid and L-tyrosine, are recognised by the respective receptors of the GerA family (located in inner membrane), a series of biophysical events are initiated[50]. This involves the release of monovalent ions from the core (H^+, Na^+, K^+) followed by the release of high amounts of Ca^{2+}-DPA, resulting in partial core hydration[50,54]. The lytic enzymes from the cortex, possibly Sleb and ClwJ[54,55], are then activated, which seems to be a critical step for germination. Through degrading the cortex from

opposite sides - SleB from the inside out and CWIJ from the outside - they allow expansion and total rehydration of the core[54]. This will enable the reactivation of metabolic activity and the synthesis of macromolecules[50]. Subsequently, the activity of the proteases together with the core swelling culminates in the mechanical disruption of the spore coat, allowing the outgrowth of the vegetative cell[50,54].

P. larvae spore's germination only occurs in the larval gut, where L-tyrosine and uric acid are combined, and remain dormant in adult bees' gut, where the germinating agents are spatially separated. It is worthing note that germination responses in different *P. larvae* strains are similar[17,19].

Considering that AFB symptoms are only evident after disease outbreak, the focus of some research has been the monitoring of *P. larvae* spore load in hive, known to be positively correlated to the likelihood of occurring clinical symptoms[2,26]. While Gende and colleagues (2011) suggested that a level of around 3000 spores per adult bee is the threshold for the onset of the first symptoms of AFB[26], Stephan *et al.* (2020) reported only an average of 228 spores per bee[2].

As already mentioned, besides highly contagious and difficult to eradicate, once established in the hive it will cause the death of the entire colony. Therefore, the early detection of spores in adult bees is particularly important for asymptomatic colonies - about 25 % of spore-producing colonies remain undetected[2] -, since may help to prevent this disease and consequently contribute to the implementation of prophylaxis or controlling sanitary measures.

1.6. Current methods for *P. larvae* detection

Currently, AFB diagnosis is based on the identification of the etiological agent and on the observation of clinical symptoms[6]. The latter depends on the genotype involved, the stage of the disease and the strength of the bee colony[57].

According to the World Organization for Animal Health, the current detection techniques used to isolate and identify *P. larvae* require: (a) a previous culture step, and only then the bacteria can be identified through conventional polymerase chain reaction (PCR), mass spectrometry, biochemical tests, antibody-based techniques and microscopy; or (b) can be directly performed on collected samples through real-time PCR (qPCR).

The culture-based detection techniques used to isolate and identify *P. larvae* are slow (requires several days) hindering treatment due to a time-consuming turnover[58,59]. Moreover, the results depend on the culture medium with a high probability of false negatives arising in a certain environment[60]. **Table 3** shows the test methods available for monitoring AFB disease in hives.

Table 3. Methods available for the monitoring AFB disease in hives without visible clinical symptoms. Adapted from Word Organization for Animal Health (2019)

Method	Previous culturing step	AFB monitoring
Bacterial isolation	Yes	+++
Mass spectrometry		-
Antigen detection		++
Microscopy		++
Conventional PCR		+++
Real-time PCR	No	+++
Vita Bee Health Kit		++

+++ recommended method; ++ suitable method; - inappropriate method for the purpose

Molecular methods, such as PCR-based ones, have overcome many culture-based limitations due to their specificity, high sensitivity and cultivation avoidance[16,60,61]. In the last year, Crudele and co-workers (2019) compared qPCR with culture-dependent methods to detect *P. larvae* spores in honey, concluding that the second led to false-negative results (59.6 % positive samples by qPCR versus 32.3 % with plate count[60]). Nonetheless, the efficiency of DNA recovery, the influence of inhibitors in PCR reaction from sample matrix, and the false-positive results due to dead bacteria DNA might compromise this molecular method[62,63]. Furthermore, and similarly to immunoassays, PCR does not distinguish between viable and non-viable bacterial cells[58].

The use of antibodies for detecting vegetative cells is also being explored, but it brings some disadvantages such as: complex, time-consuming and expensive production; sensibility to temperature and pH; and propensity to aggregation[2,14]. Yet, the lateral flow device developed by Vita Europe Ltd. – Vita bee Health kit - uses antibodies and allows to detect ERIC I strains of *P. larvae* in the vegetative state, on-site[64].

Based on this, new methods able to overcome the existent drawbacks will play a critical role in *P. larvae* control.

Recently, Santos *et al.* (2019) revealed the sequence of a cell wall binding domain (CBD) derived from lysin PlyPl23[25] able to specifically bind to *P. larvae* of all ERIC genotypes. As a recognition element, this CBD was been reported as having a high potential for *P. larvae* detection[14].

1.7. Current methods for *P. larvae* spore's purification

The early detection of subclinical *P. larvae* infection would largely benefit from a faster spore detection methodology. When vegetative cells are identified by the conventional methods the AFB outbreak may already been started[6,65]. A method for the purification and concentration of spores directly from the samples collected on field (adult bees) may be challenging to develop.

Mahdi *et al.* (2018) described a protocol for this purpose in which HistoDenz® gradient was used: 50 % (w/v) and 20 % (w/v). After centrifugation, the pellet contain the dormant spores, the intermediate phase the germinating spores and the upper phase, the cellular debris (**Figure 6**).

Figure 6. General scheme of dormant spores' separation from other components (cells, cells debris and germinating spores) by HistoDenz® gradient.

These protocols were optimized with ERIC I genotype strains, thus some parameters may have to be adjusted concerning others ERIC genotypes. Despite the method allows obtaining stocks of spores with a high degree of purity[10,12,66], it is a sensitive method with associated loss of spores.

As such, the development of more expeditious methods allowing spore purification and concentration from bee samples would be highly valuable to support new spore-detection methods.

Currently, recombinant hybrids containing a polypeptide fusion partner, called affinity tag, are widely used to facilitate target purification. Moreover, several different proteins, domains or peptides can be fused depending on the purpose[67]. The advantages of using fusion proteins to facilitate the purification, detection or improvement of various targets are well recognized[67]. For example, magnetic beads coated with CBDs have already been reported for pathogen immobilization, separation and detection from complex matrix with higher recovery rates[42,68]. Yet, the CBD binding to spores might be prevented by spore coat. As no information about spore-affinity molecules have ever been reported for *P. larvae,* the ability of fusion proteins to bind to *P.larvae* spores has never been explored. Nevertheless, considering the similarity between *Bacillus subtilis* and *Paenibacillus larvae*[60], we can expect the presence of common proteins in the spore coat of each one of them – it is far known the presence of keratin-like in the spore coat of *B. subtilis*.

In 2019, Tinoco and colleagues showed the improvement of the thermal properties of hair by the binding of human crystallin (Cryst) conjugated with a keratin-based peptide (KP). Besides the high thermal stability of the KP-Crystallin (KP-Cryst) fusion protein, a relatively good hair binding at different pH has also been demonstrated. Thus, in the present work we took advantage of the KP-Cryst fusion protein developed by Tinoco et al.(2019)[67] to create a novel method of capturing *P. larvae* spores - relying on the thermodynamic stability of Cryst (provided by the extremely strong packaging of its β-sheet Greek key motifs and their respective interactions) with the ability of a KP to bind to keratin-like proteins, presumably present in the spore coat of *P. larvae.*

1.8. Aim

AFB is the most lethal bee disease in the world, caused by the gram-positive bacteria *P. larvae*. Currently, the existing methodologies for the detection and identification of this bacterium present several deficiencies. Some are highly time consuming, while the effectiveness of others may be compromised by several factors.

For those reasons it is urgent to find new methods allowing faster analysis with high accuracy.

The purpose of this work is to develop a rapid method for early AFB detection, ideally with potential to be applicable *on site* and with final results within 24 h or less. Accordingly, it shall not comprise centrifugation steps and it must assure a high spore recovery efficiency, where a spore loss equal or inferior to 1-Log is the main target.

For that, the use of KP-crystallin (KP-Cryst) fusion protein to effectively recover and concentrate *P. larvae* spores was planned, to allow the subsequent use of a phage lysin CDB (of PlyPl23) that would specifically bind to *P. larvae* after induced spore germination.

Chapter 2. Methodology

2.1. Expression, purification and quantification of PlyPl23 CBD

The expression of the PlyPl23 CBD (CBD) was performed as described by Santos *et al.,* (2019)[14]. Briefly, a single colony of the mutant with the recombinant plasmid was inoculated in Lysogeny Broth (LB) medium supplemented with 50 μg.mL^{-1} of kanamycin and grown *overnight* at 37 °C. Then, a certain volume (1:10) of the pre-inoculum was inoculated into LB medium supplemented kanamycin until reaching an optical density at 620 nm (OD_{620nm}) of 0.5. The recombinant protein expression was induced with isopropyl-ß-D-thiogalactopyranoside 1 mM, and performed *overnight* at 16 °C, 150 rpm. The cells were harvested by centrifugation (8 000 ×*g*) for 10 minutes (min) and then resuspended in 1/25 volume of lysis buffer (20 mM NaH_2PO_4, 500 mM sodium chloride, 10 mM imidazole, pH 7.4). The cellular rupture was performed by freeze-thawing (3 cycles, from -80 °C and bain marie at 37 °C), followed by 6 min of sonication (Cole-Parmer Ultrasonic Processor) during 10 cycles (30 s ON, 30 s OFF) at 30 % amplitude. Soluble cell free extract was separated by centrifugation (9 500 ×*g*, 30 min, 4 °C), filtered (0.22 μm PES membrane) and loaded on a 1 mL HisPur™ Ni-NTA Resin (Thermo Scientific) stacked in a Polypropylene column (Quiagen). After two washing steps with protein-dependent imidazole concentrations (lysis buffer supplemented with 10 mM imidazole in the first wash, and 30 mM imidazole in the second wash) the protein was eluted with 300 mM imidazole (two fractions: 200 and 700 μl). Samples of each fraction were analysed by SDS-PAGE (**Appendix I**).

The purified protein was concentrated and dialyzed against a storage buffer (10 mM Tris-HCl, pH = 7.0) through centrifugal Amicon Ultra - 0.5 mL (Millipore) filters and stored at 4 °C. Protein concentration was determined using the BCA Protein Assay Kit (Thermo Scientific) with bovine serum albumin (BSA) as standard (**Appendix II**)

2.2. Bacterial strains

In this study, a *P. larvae* strain previously isolated from Portuguese hives was used: Pl02-27 (H27), belonging to the ERIC I genotype[25]. This strain, stored at -80 °C with 20 % glycerol, was cultivated in MYGPG agar (10 g.L^{-1} Mueller-Hinton Broth (Oxoid); 15 g.L^{-1} yeast extract (Oxoid); 3 g.L^{-1} de K_2HPO_4 (LabKem); 1 g.L^{-1} de Sodium-pyruvate (Fisher); 2 % glucose (Ameresco) and 17 g. L^{-1} agar (VWR)) and incubated for two days at 37 °C under 5 % CO_2.

2.3. *P. larvae* spore's preparation

P. larvae spore's suspensions were prepared based on the procedure described by Oliveira *et al.* (2015)[25], with some modifications. Briefly, strain H27 was spread over MYPGP agar and then incubated, at 37 °C under 5 % CO_2 for 8 days. Ice cold ddH_2O water was poured onto the bacterial lawns, which were scrapped from the MYPGP agar plate, and the suspension obtained was then collected Spores were pelleted by centrifugation (8 000 ×*g*, 5 min) and suspended in fresh dd$H_2$0. After three washing steps with sterile water, spores were purified following a methodology described by Mahdi *et al.* (2018)[10]. In this procedure a two-phase aqueous system was used, composed of HistoDenz®. A two-phase gradient was created by adding a 20 % (w/v) to a 50 % (w/v) HistoDenz® solution, dissolved in water (total volume of 5 mL), allowing the separation of phases. Afterwards, 4 mL of spores' suspension and 1 mL of sterile water (total volume of 5 mL) were carefully poured on the top layer and centrifuged at 7 400 ×*g* for 35 min (4 °C). Next, the last 2.5 mL of the lower phase (where spores were concentrated) was carefully recovered. Spores were washed three times (12 000 ×*g*, 2 min) and resuspended in 1 mL ddH_2O.

The purification efficiency was determined by microscopy (Olympus BX51, 1000x magnification) to verify the presence/absence of vegetative cells.

The spore concentration (CFU.mL^{-1}) was assessed as follows: 20 µl of spore's suspensions were heat activated (75 °C, 15 min), serially diluted in sterile dd$H_2$0, and spread over MYPGP agar. Plates were incubated for 2 days at 37 °C, 5 % CO_2.

2.4. Germination assays

The binding ability of CBD on germinating spores of H27 was determined. Spores were firstly decoated: 100 µl of each spore's suspensions were centrifuged (12 000 ×*g*, 2 min) and then resuspended in 50 µl of dithiothreitol (DTT, 100mM) and 50 µl Proteinase-k (1 mg.mL^{-1}). After an incubation of 40 min at 56 °C, 5 µl of lysozyme (0.05 mg.mL^{-1}) was added and the mixture was incubated for another 20 min at the same conditions. After three washing steps (12 000 ×*g*, 2 min, 4 °C) with sterile water, the spores pellet was incubated with germinants, which consisted in a solution of 80 µl MYPGP, 10 µl L-tyrosine (3 mM) and 10 µl uric acid (3 mM), and incubated at 37 °C under 5 % CO_2 (120 rpm) for 4 h. After centrifugation, the pellet was resuspended in 100 µl of NaCl. Next, suspension was harvested and 15 µl of CBD (10 µM) was used to resuspend the pellet. After 20 min of incubation at room temperature (rt),

two washing steps with sterile NaCl 0.9 % were made. At last, pellet was resuspended in a residual volume of sterile NaCl 0.9 %.

The effectiveness of the binding assay was determinate by fluorescence optical microscopy (FOM) - Olympus BX51, Magnitude 1000x - comparing the images from bright field with the ones obtained under FITC filter. Dormant spores and vegetative *P. larvae* cells were used as negative and positive control, respectively.

2.5. Expression, purification, and quantification of KP-Crystallin

The expression of the KP-Cryst was performed as described by Tinoco *et al.,* (2019)[67]. Briefly, a single colony of the mutant with the recombinant plasmid was inoculated in LB supplemented with kanamycin and grown *overnight* at 37 °C. A certain volume (1:10) of the pre-inoculum was inoculated into Terrific Broth–Auto Induction Medium. The culture was grown for 24 h at 37 °C, 200 rpm. The cells were harvested by centrifugation (7 000 ×*g* at 4 °C for 5 min) and then resuspended in phosphate buffer (20 mM sodium phosphate, 500 mM sodium chloride, 10 mM imidazole, pH 7.4) with a protease inhibitor. The cellular rupture was performed by sonication (vibra-cell™ SONICS) for a total of 10 min (3 s ON, 9 s OFF) at 40 % amplitude. The soluble cell free extract was separated by centrifugation (10 000 ×*g*, 40 min, 4 °C), filtered (0.22 µm PES membrane) and loaded on a 1 mL HisPur™ Ni-NTA Resin (Thermo Scientific) stacked in a Polypropylene column (Quiagen). After four washing steps with protein-dependent imidazole concentrations (phosphate buffer supplemented with 20 , 40, 50 and 80 mM imidazole in the first, second, third and fourth wash, respectively) the protein was eluted with 100 (one elution), 250 (one elution) and 500 mM imidazole (three elution). Samples of each fraction were analysed by SDS-PAGE (**Appendix III**).

The purified protein was concentrated and dialyzed against a storage buffer A (120 mM Heppes, 500 mM NaCl, pH 7.0) through centrifugal Amicon Ultra - 0.5 mL (Millipore) filters and stored at 4 °C. Protein concentration was determined using the BCA Protein Assay Kit (Thermo Scientific) with BSA as standard.

2.6. FITC Linkage to KP-Cryst

To study the adhesion profile of KP-Cryst to dormant spores and its ability to coat nickel magnetic beads, fluorescein 5(6)-isothiocyanate (FITC) was linked to the protein. The staining of the KP-Cryst with

FITC was performed as described by Tinoco *et al.,* (2019)[67]. The protein was dissolved in 0.1M sodium carbonate buffer, pH 9, at 1 $mg.mL^{-1}$. A volume of 5 mL from these solutions was incubated with 250 µL of a 0.5 $mg.mL^{-1}$ FITC in DMSO solution, at 4 °C. Unbound FITC was separated from the conjugate KP-Cryst-FITC by dialysis against water, at 4 °C.

2.7. Functionalization of Magnetic Beads

Nickel magnetic beads (MB) - Ni-Charged MagBeags from GenScript - with strong metal-chelating agent suitable for binding of six His-tags were used. A volume of 15 µl of the provided suspension was incubated with KP-Cryst (0.07 $mg.mL^{-1}$) for 1 h at room temperature (rt) and deprived from light (DL). MB were then collected using a magnetic support and washed twice with ddH_2O water. The number of MB used in each assays was estimated based on Loessner *et al.* (2007) – **Appendix IV** - using the following formula: $[4/3\ \pi r^3] \times 0.28$, where r represents the average radius of MB.

The effectiveness of the binding assay was confirmed by FOM (Olympus BX51, Magnitude 1000x), comparing the images in bright field and under the FITC filter. MB alone were used as negative control.

2.8. KP-Cryst non-specific binding

Homogenised bee's mid-hind guts (HBG) were prepared and incubated with KP-Cryst to evaluate the protein non-specific binding. Briefly, 10 bees were washed in 0.9 % NaCl, dissected with a sterile tweezer, and the bee's mid-hind gut were collected to a microtube. After the addition of 30 µl of ddH_2O, the solution was vigorously vortexed, centrifuged at 8 000 $\times g$ for 5 min, and the supernatant was collected. Each HBG was treated in triplicate: (a) without heat treatment; (b) with heat treatment at 80 °C for 10 min; (c) with heat treatment at 95 °C for 3 min. Next, labelled KP-Cryst (0.07 $mg.mL^{-1}$) was added to each sample and incubated at rt for 20 min, DL. After three washing steps (8 000 $\times g$, 5 min) each solution was resuspended in 20 µl of ddH_2O. HBG alone were used as negative control to monitor the tissue autofluorescence.

KP-Cryst non-specific binding to bee commensals, namely *P. larvae*, was also tested using the H27 strain. After cultivation, one single colony of this strain was resuspended in 500 µl of NaCl 0.9 %. Then, the bacterial suspension followed the same procedures adopted for the HBG.

The effectiveness of the binding assay was determinate by FOM (Olympus BX51, Magnitude 1000x) comparing the images in bright field and under the FITC filter.

2.9. KP-Cryst binding to spores

A spore suspension (10^8 CFU.mL^{-1}) was incubated with 0.07 mg.mL^{-1} KP-Cryst at rt, DL. Incubation times were 10, 15, 20, 25 and 30 min. After three washing steps (12 000 ×*g*, 2 min), pellet was resuspended in a residual volume of ddH_2O.

In order to access if KP-Cryst binding to spores (KP-Cryst-Sp binding) was affected by the presence of HBG (no heat), 20 µl of the latter, either no-filtered and filtered (through 0.45 µm), were added to a suspension of 20 µl of spores (10^8 CFU.mL^{-1}). Next, KP-Cryst (0.07 mg.mL^{-1}) was added to the mixture, with incubation occurring at rt for 20 min, DL. After three washing steps (12 000 ×*g,* 2 min) each pellet was resuspended in 20 µl of ddH_2O.

The effectiveness of the binding assay was inferred by FOM (Olympus BX51, Magnitude 1000x) comparing the images in bright field and under the FITC filter.

2.10. Influence of KP-Cryst superficial charge on KP-Cryst-spores binding

2.10.1. Dynamic Light Scattering (DLS)

The zeta potential (mV) of a pure suspension of spores (10^6 CFU.mL^{-1}) in water was determined on a Zetasizer Nano ZS (Malvern Instrumentts), with a Zetasizer software. The data was recorded according to the viscosity of water at 25 °C: 0.893 x 10^{-3} Pa.s.

2.10.2. Efficiency of positively charged KP-Cryst in binding to spores

The influence of the charged KP-Cryst on binding to spores was evaluated using buffer A (pH 7) and buffer B (pH 5), through protein quantification and by confocal microscopy.

a) Protein quantification

The protein (initial concentration, Ci = 0.4 mg.mL^{-1}) was incubated with two pure spore suspensions at different initial concentration ([Sp]$_i$ -CFU.mL^{-1}) - 10^7 and 10^5 CFU.mL^{-1} - for 20 min at rt. After a centrifugation step (12 000 $\times g$ for 2 min), the supernatant was collected and the unbound protein (UP) was quantified using the BCA Protein Assay Kit. The quantity of KP-Cryst bound to spores (Cf) was assessed through the following formula: Cf = Ci-UP.

The binding efficacy (%) was determined as follows:

Binding efficacy=[Cf/Ci] x 100.

b) Confocal microscope

The high quality and definition of the Confocal images would enable the use of software capable of analysing the fluorescence intensity of different areas of the image, simplifying the comparison of the intensity of KP-Cryst-Sp binding at different pH's. So, for confocal microscopy, KP-Cryst (0.4 mg.mL^{-1}), either positively charged (suspension in buffer B) or neutral (suspension in buffer A), was used to resuspend a pellet of spores (10^7 CFU.mL^{-1}). The 20 min incubation (DL at rt) was followed by two washings (12 000 $\times g$, 2 min), and the pellet was finally resuspended in 25 µl of the respective buffer.

The analysis was performed using the Confocal Scanning Laser Microscope (Olympus BX61, FluoView 1000 model). For all samples, the image acquisition was done using the same settings (filter, exposure time and luminosity). The detection was obtained with a laser excitation line at 488 nm and emission filters BA 505-605, green channel. The images were acquired with the FV10-Ver4.1.1.5 (Olympus) programme.

The digital image analysis, namely determination of Corrected Total Cell Fluorescence (CTCF), was enabled by the use of Image j software (imagej.nih.gov/ij).

2.11. MB saturation by KP-Cryst

Different KP-Cryst concentrations - 0.50, 0.75 and 0.90 mg.mL^{-1} - were evaluated with MB (20 µl), and incubation was performed for 1 h at 4 °C, with 50 rpm, and DL. MB were then separated from supernatant (contains UP) using a magnetic column, and washed twice.

The determination of UP (mg.mL^{-1}) present in the supernatant after magnetic separation was obtained by protein quantification, using the formula described above - **Section 2.10.2**. MB saturation was then assessed. According to MB manufacturers' instructions, knowing that 1000 µl of MB can capture 40 mg of His-tags proteins, 20 µl of MB can capture (MB-Cap):

MB-Cap (mg) = ([Vi (MB) x 40 mg] / 1000 µl) = (20 x 40 / 1000) = 0.8 mg of KP-Cryst. Thus, for 20 µl of MB, the capture of 0.8 mg of KP-Cryst correspond to 100 % of MB saturation.

The effectiveness of the binding assay was then confirmed by FOM (Olympus BX51, Magnitude 1000x).

2.12. Spore capture and *P. larvae* detection through MB functionalised with KP-Cryst

The spore recovery and subsequent *P. larvae* detection can be divided in three major phases: (A) beads functionalization with KP-Cryst (MB-KP-Cryst); (B) spore capture (MB-KP-Cryst-Sp); (C) *P. larvae* detection. A general representation of the MB-KP-Cryst-Sp-CBD system (spore capture and detection system) is shown in **Figure 7**.

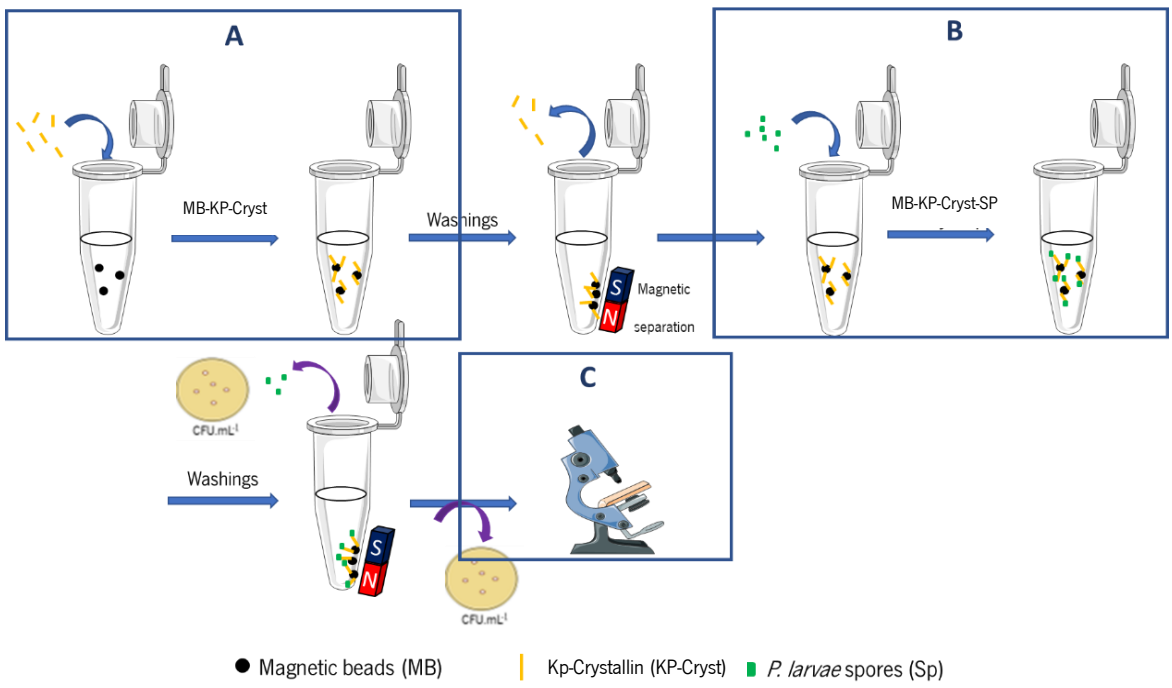

Figure 7. General representation of MB-KP-Cryst-Sp-CBD system, which allows the spore recovery by MB functionalized with KP-Cryst, with subsequent *P. larvae* detection by CBD.

Briefly, MB were first functionalized with KP-Cryst, leading to the formation of MB-KP-Cryst complex (A). The complex was then collected with a magnetic stand (for the removing of UP) and washed twice. Next, a certain volume of spores was added to the system, occurring the formation of MB-KP-Cryst-Sp complex at rt (B). Following the washings with a magnetic stand – to remove unbound spores (US) -, in order to evaluate the spore capture by the system, a certain volume of MB-KP-Cryst-Sp was plated for subsequent CFU.mL^{-1} counting. At the same time, unbound spores were also plated in order to determine spores not captured by the complex MB-KP-Cryst. Finally, (C) spores were dissociated from beads by decoating (decoating disrupted the bounding between KP-Cryst and spores), which was followed by germination and subsequent detection by CBD, as already described **(Section 2.4.)**.

It is important to note that: (i) some assays were performed in the presence of HBG, where the latter and spores were equally mixed and added to the system; (ii) spores for CFU counting were serial diluted and spread over MYPGP agar plates, and incubated for 2 days at 37 °C, 5 % CO_2 (all CFU counts were performed in triplicate, where the results are presented as mean ± SD); (iii) protein quantification of UP was performed after MB-KP-Cryst incubation in some assays; (iv) for $[Sp]_i$ = 5-Log, the ratio MB-KP-Cryst : spores (MB-KP-Cryst : Sp) was varied in the last assays. In this way, a series of process variables have been changed throughout the process in order to optimize the spore capture by the system. **Table 4** describes the conditions used in each assay.

Table 4. Representation of the conditions used in each MB-KP-Cryst-Sp-CBD system.

N° MB	KP-Cryst ($mg.mL^{-1}$)	MB-KP-Cryst incubation	UP quantification	$[Sp]_i$ ($CFU.mL^{-1}$)	HBG	MB-KP-Cryst-Sp	CBD adding
1.5×10^5	0.07	1h; rt; 50 rpm; in buffer A	No	8-Log	Yes	1h 30 min; rt; 50 rpm; in HBG	No
					No	1h 30 min; rt; 50 rpm; in water	
	0.2	1h; 4 °C; 50 rpm; in buffer A				20 min; rt; 50 rpm; in water	
	0.4	1h; 4 °C; 50 rpm; in buffer A		5-Log		1h 30 min; rt; 50 rpm; in water	
				7-Log			
				5-Log		1h 30 min; rt; 50 rpm in buffer B	
				7-Log			
		1h; 4 °C; 50 rpm; in buffer B	Yes	5-Log		1h 30 min; rt; 90 rpm; in buffer B	
				7-Log	Yes	1h 30 min; rt; in HBG	
1.67×10^5	0.75			5-Log*	No	1h 30 min; rt; 50 rpm; in buffer B	
				7-Log	Yes	1h 30 min; rt; 50 rpm; in HBG	
					No	1h 30 min; rt; 50 rpm; in buffer B	Yes

*Three assays were performed with different ratios of MB-KP-Cryst : Sp (number of MB/CFU of spores) - 1, 10 and 20.

2.13. Colony polymerase chain reaction (ID colony PCR)

Given that (i) the MB, although previously washed, could still contain bacterial contamination and (ii) the HBG contains several microorganisms: the CFUs obtained by plating the suspensions collected

throughout the process (theoretically containing captured spores and US), were identified as *P. larvae* by ID colony PCR based on 16S rRNA gene. For that, first, each selected colony was resuspended in 10 µl grade water. Next, PCR reactions by using PL1 and PL2 primers[49] were set up as 25 µl mixtures containing: 1 µl DNA template; 2 µl of PL1 (forward) and PL2 (reverse) primers; 12.5 µl of XPert FasterMix (2x dye) Taq polymerase; 7.5 µl of grade water. The following PCR conditions were used: a 95°C (15 min) denaturation step; 40 cycles of annealing at 93 °C (1 min), 55 °C (35 seconds), and 72 °C (1 min); and a final cycle of extension at 72°C (5 min). Then, the PCR products were submitted to electrophoresis in a 0.8 % agarose gel until the dye migrated as far as 2/3 length. Gels were visualized in a Molecular Image ChemiDoc TM XRS + Imaging System (Bio-Rad) and analyzed using the Image Lab 4.0 software (**Appendix V**). Fragment sizes were inferred utilizing the GRS Universal ladder (grisp) DNA molecular weight marker, which produces a pattern of 15 spaced bands, ranging from 100 to 10 000 bp.

2.14. Statistical analysis

Data were analysed using Prism 8 software (GraphPad, CA, USA) where *p-value* and statistically significance were generated by *t-test* **(Section 3.5.3.a. - Evaluation of KP-Cryst-Sp binding with pH)** and *One-way ANOVA* **(Section 3.5.4. – Optimizing spore recovery from low-concentrated suspensions)**. Means and standard deviations (SD) were determined for independent experiments and results were presented as mean ± SD. For all tests a confidence level of 95 % was used.

Chapter 3. Results

In this work, *P. larvae* was detected through binding to the previously reported PlyP23 CBD[14]. The presence of green-decorated cells visualised under fluorescence microscopy (FITC filter) were indicative of a positive result. But the success of this detection depended directly on an effective capture of spores from samples. Functionalized MB-KP-Cryst were used, relying on the KP-Cryst's ability to bind to spore keratin-like proteins[67].

3. *P. larvae* detection and spore capture

3.1. Evaluation of CBD binding to *P. larvae* germinating spores

After confirming the absence of vegetative cells on spore suspension, the CBD's ability to attach to germinating spores was assessed. For this, the dormant spores were decoated and subsequently its germination was induced. The CDB was then added to the germinating spores, and their binding analysed by FOM (**Figure 8**)

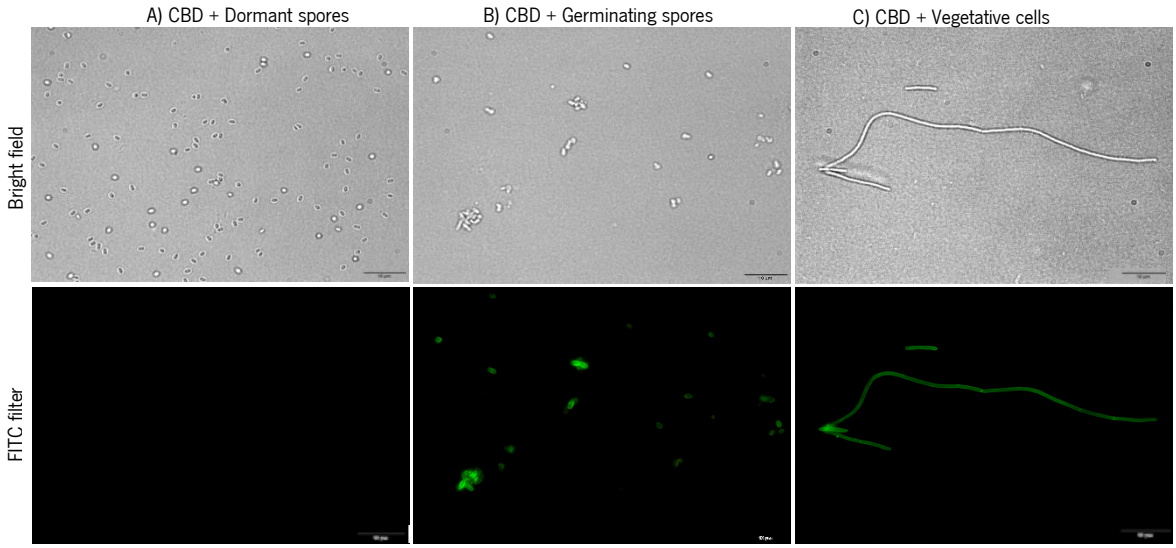

Figure 8. *P. larvae* spores and vegetative cells decorated with CBD. (A) CBD with dormant spores, acting as a negative control; (B) CBD with germinating spores using an exposition time of 400 ms; (C) CBD with H27 vegetative cells using an exposition time of 100 ms, acting as a positive control.

The observation of more elongated and green-decorated spores revealed the CBD's ability to bind to germinating spores. Nevertheless, the positive control showed that the binding of CBD is stronger to vegetative cells compared to germinating spores, as exposure times observed were 100 ms and 400 ms respectively. The negative control showed that CBD cannot bind to dormant spores.

3.2. KP-Cryst's expression, purification and binding to MB

In order to confirm MB-KP-Cryst binding, 0.07 mg.mL^{-1} of KP-Cryst were incubated with 1.5x10^{5} MB for 1h at rt. The result of the binding is shown in **Figure 9.**

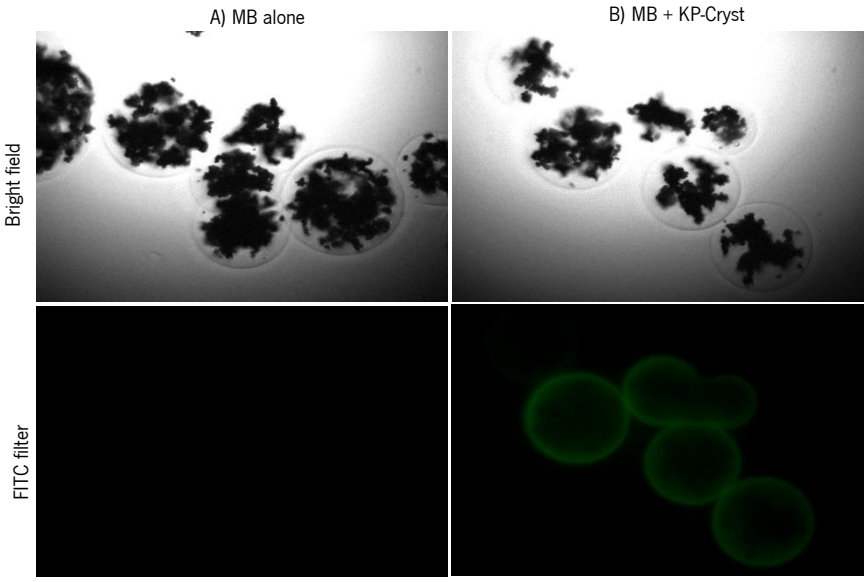

Figure 9. MB coating by KP-Cryst. (A) MB alone acting as negative control; (B) MB with 0.07 mg.mL^{-1} of KP-Cryst. Images obtained with 200 ms of exposition time.

By comparing the MB before (A) and after (B) incubation with KP-Cryst, the differences were clearly visible. While the negative control shows that MB have no autofluorescence, the appearance of green-decorated MB indicates that MB-KP-Cryst binding was successful. Nevertheless, not all the MB that appear in the bright field were fluorescent with FITC. The fast deposition of the MB observed during the assay might be the cause of this observation, and based on it, subsequent incubations involving MB (MB-KP-Cryst and MB-KP-Cryst-Sp) occurred with agitation (50 rpm).

3.3. Evaluation of KP-Cryst non-specific binding

The non-specific binding of KP-Cryst has firstly analysed in HBG (simulating real samples). And then in *P. larvae* vegetative cells. After incubation with the protein for 20 min at rt, samples were washed and observed under FOM, through FITC filter (**Figure 10**).

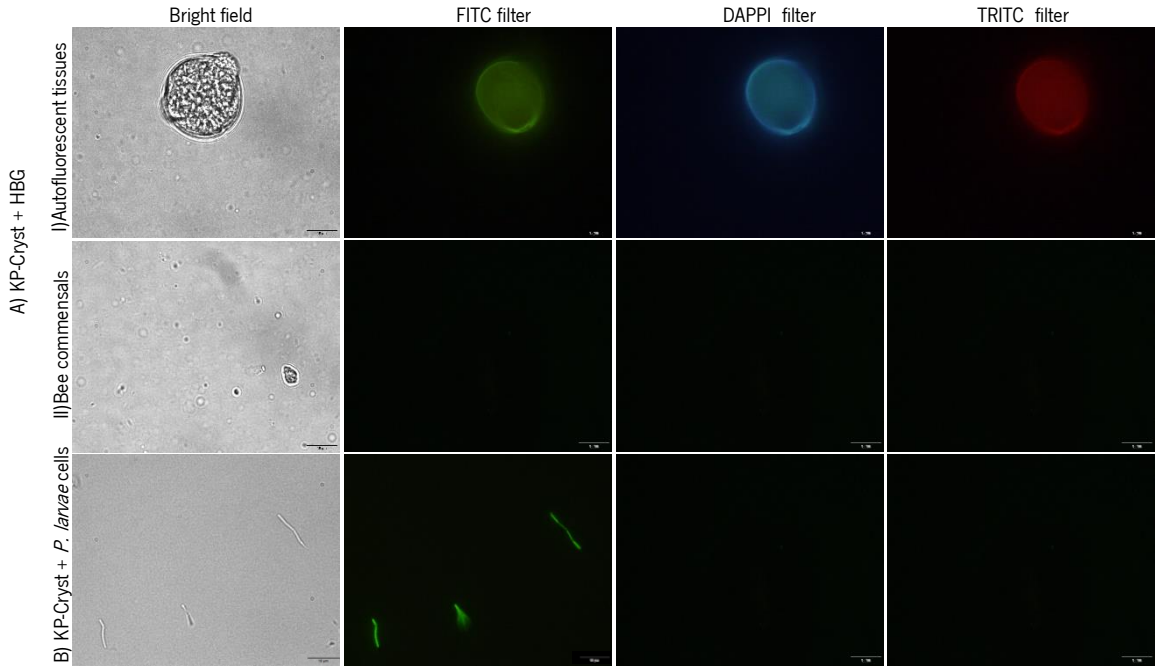

Figure 10. KP-Cryst non-specific binding. (A) KP-Cryst with HBG: A.I - Autofluorescent tissues of HBG; A.II - Bee commensals with no affinity to KP-Cryst; (B) *P. larvae* vegetative cells green-decorated with KP-Cryst using an exposition time of 100ms.

The fluorescence observed with FITC filter was also present in the images captured with the TRITC and DAPPI filters, from the same microscopic field, indicating that the fluorescence was not due to KP-Cryst FITC, but to the tissue autofluorescence (**Figure 10.A.I**). Moreover, the visualization of several not green-decorated bee commensal cells, indicates that KP-Cryst has no affinity to them **(Figure 10.A.II)**. Opposingly, the observation of *P. larvae* green-decorated cells only with FITC filter confirmed KP-Cryst's binding (**Figure 10.B**)

In order to determine whether cellular rupture could prevent KP-Cryst from attaching to *P. larvae* cells, prior to incubation with the protein these cells were pre-heated to different temperatures: 80 °C and 95 °C, for 10 and 3 min, respectively. **Figure 11** shows the result of the KP-Cryst binding to the pre-heated cells.

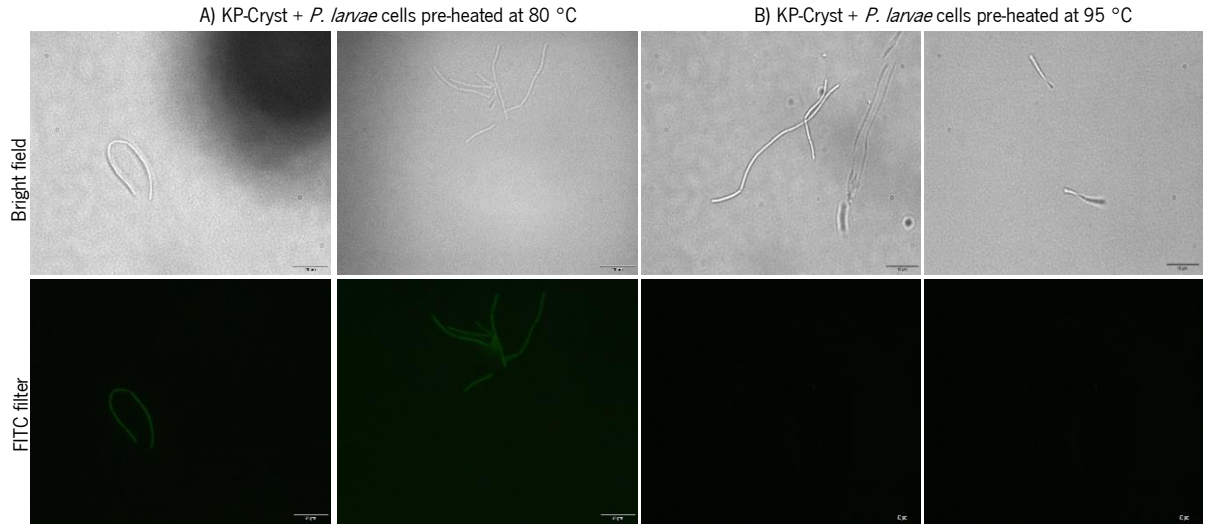

Figure 11. KP-Cryst binding to pre-heated *P. larvae* vegetative cells. (A) Vegetative cells pre-heated at 80 °C for 10 min; (B) Vegetative cells pre-heated at 95 °C for 3 min. Images obtained with an exposition time of 250 ms.

From the analysis of the **Figure 11**, it can be said that the heat treatment at 80 °C didn't prevent the protein binding, as cells were green. Regarding heat treatment at 95 °C, no binding was detected in the microscopic field.

3.4. Evaluation of KP-Cryst binding to *P. larvae* spores

3.4.1. KP-Cryst-Sp binding

A volume corresponding to 0.07 mg.mL^{-1} of KP-Cryst was added to a pure pellet of concentrated spores ($[Sp]_i$ = 8-Log), and five different incubation times were evaluated: 10, 15, 20, 25 and 30 min. Despite green-decorated spores were observed for all the time points, different exposure times were used in these observations: 400 ms for incubations of 10 and 15 min, and 200 ms for 20, 25 and 30 min. The lower incubation time with higher exposure time was used in the subsequent experiments: 20 min. **Figure 12** shows KP-Cryst binding for 10 and 20 min of incubation with the same exposure time.

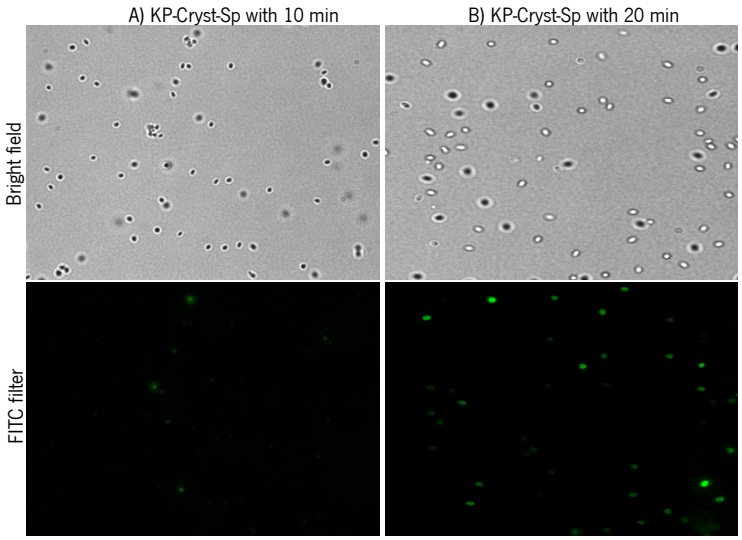

Figure 12. *P. larvae* spores decorated with KP-Cryst. (A) KP-Cryst-Sp binding for 10 min; (B) KP-Cryst-Sp binding for 20 min. Images obtained with an exposition time of 200 ms.

3.4.2. KP-Cryst-Sp binding in HBG

KP-Cryst-Sp binding was assessed in artificially contaminated HBG, simulating real samples. HBG and spores were incubated with the 0.07 $mg.mL^{-1}$ KP-Cryst for 20 min for further FOM analysis (**Figure 13**).

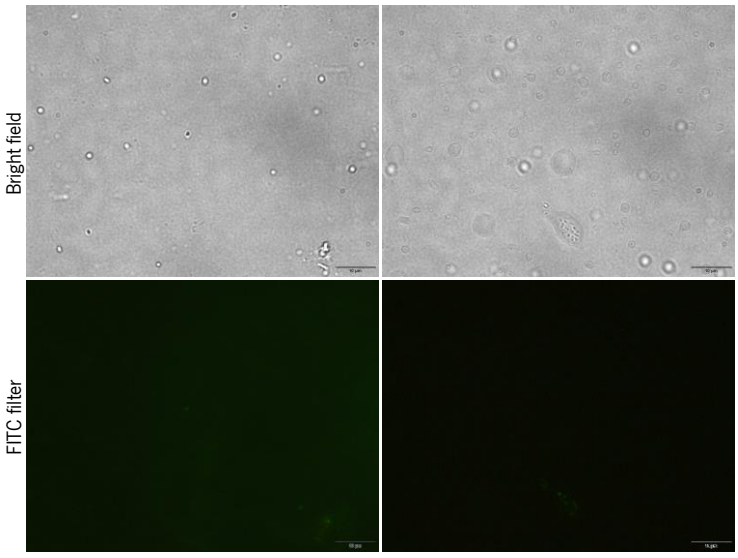

Figure 13. KP-Cryst-Sp binding in HBG. Images obtained with an exposition time of 1000 ms.

It was observed that no spores were fluorescent with FITC filter, indicating a negative influence of the HBG on KP-Cryst-Sp binding.

In an attempt to overcome this, prior to infection with spores, the HBG was filtered through 0.45 µm. The experiment was repeated with this new variable, revealing that almost all spores in the microscopic field were green-decorated. Nevertheless, higher exposure times were required comparatively to spores in water– 1000 ms and 200 ms, respectively, and even so, with less fluorescence intensity (**Figure 14**).

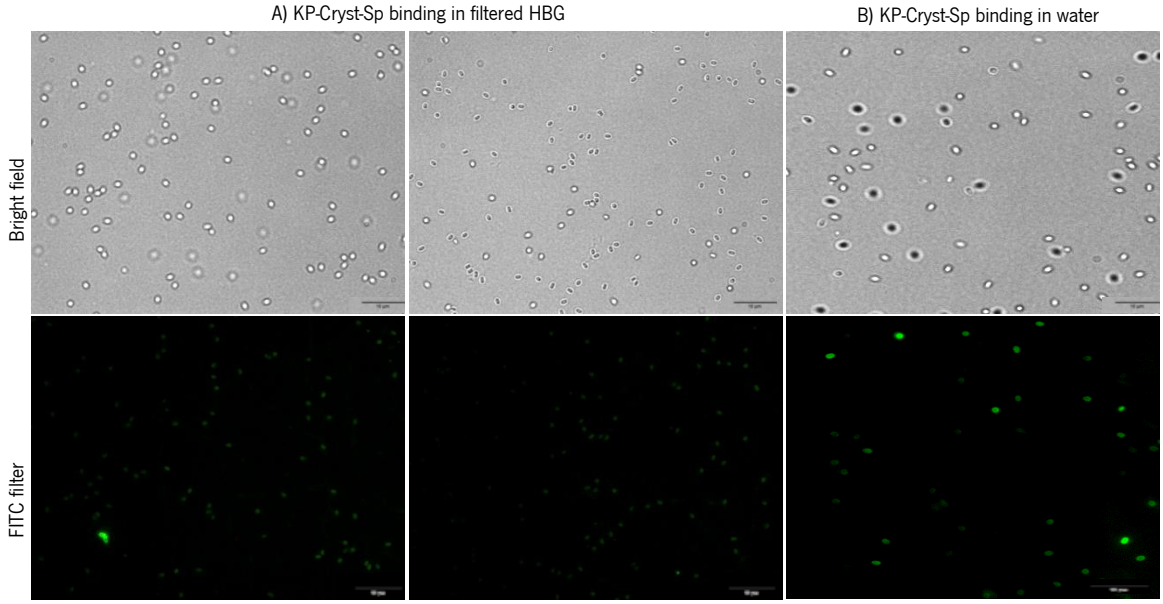

Figure 14. KP-Cryst-Sp binding in different environments. (A) KP-Cryst-Sp in filtered (cut-off of 0.45 µm) HBG (image obtained with 1000 ms of exposition time); (B) KP-Cryst-Sp in water (image obtained with an exposition time of 200 ms).

The pre-filtration of the HBG was then adopted in further experiments.

3.5. Optimisation of the MB-KP-Cryst-Sp system

3.5.1. Spore capture through MB-KP-Cryst-Sp, using decoating in spore dissociation from MB-KP-Cryst

a) Spore capture in water

In the first attempt of using MB-KP-Cryst-Sp for spore recovery, the decoating for the dissociation/detachment of spores from MB-KP-Cryst was evaluated. This process was expected to start removing the coat from spores previously bound to MB-KP-Cryst. Based on previous results, (i) 0.07 $mg.mL^{-1}$ KP-Cryst and $1.5x10^{5}$ MB were used, and (ii) MB-KP-Cryst binding occurred with stirring (50 rpm). **Table 5** shows the results obtained.

Table 5. Spores captured by MB-KP-Cryst-Sp system and spores undissociated from MB-KP-Cryst using decoating agents.

$[Sp]_i$ ($CFU.mL^{-1}$)	Captured ($CFU.mL^{-1}$)	Not dissociated ($CFU.mL^{-1}$)
8-Log	$3.07x10^5 \pm 1.70x10^4$	$2.13x10^4 \pm 2.62x10^3$

The comparison between captured and undissociated spores revealed that only around $2.13x10^4$ $CFU.mL^{-1}$ remained attached to MB (~10 %). Henceforth, decoating was used as dissociation agent for all the subsequent assays.

The comparison between the initial concentration of spores (10^8 $CFU.mL^{-1}$) with that captured by MB ($3.07x10^5$ $CFU.mL^{-1}$), reveal a 3-Log lost, and therefore, further experiments aimed at optimizing spore capture.

b) Spore capture in HBG

In parallel, to confirm the negative influence of filtered HBG in the KP-Cryst-Sp binding, the former was infested with spores and its capture by the complex MB-KP-Cryst was evaluated. As expected, a high spore loss was obtained: 3.4-Log.

3.5.2. Effect of KP-Cryst concentration

a) KP-Cryst concentration of 0.2 $mg.mL^{-1}$

The increase in protein concentration from 0.07 $mg.mL^{-1}$ to 0.20 $mg.mL^{-1}$ allowed a higher concentration of captured spores, $3.07x10^5$ $CFU.mL^{-1}$ and $8.31x10^5$ $CFU.mL^{-1}$, respectively (**Table 6**). This is indicative of a positive effect caused by a higher KP-Cryst concentration on MB surface.

Table 6. Effect of different KP-Cryst concentrations on spore capture.

$[Sp]_i$ ($CFU.mL^{-1}$)	KP-Cryst ($mg.mL^{-1}$)	Captured ($CFU.mL^{-1}$)
8-Log	0.07	$3.07x10^5 \pm 1.70x10^4$
	0.20	$8.31x10^5 \pm 2.46x10^4$

a.1.) Effect of MB-KP-Cryst incubation temperature

In an attempt to enhance the interaction between MB and KP-Cryst, which could result in higher spore capture, MB functionalization occurred at 4 °C instead of rt. Comparatively with previous result (spore capture of $8.31x10^5$ CFU.mL^{-1}), these new conditions allowed a higher spore recovery, $3.09x10^6 \pm 3.88x10^4$ CFU.mL^{-1}, and a loss of 1.7-Log spores. This suggests a better coating of the MB by the protein and accordingly, further MB-KP-Cryst functionalizations were performed at 4°C.

a.2.) Effect of MB-KP-Cryst-Sp incubation time

Aiming at the reduction of the total running time of the procedure, the possibility of reducing the KP-Cryst-Sp incubation time was evaluated. Based on the minimum incubation time required for an effective KP-Cryst-Sp binding (20 min), two different time periods were tested: 20 and 90 minutes ($1.5x10^5$ beads, KP-Cryst = 0.2 mg.mL^{-1}). Results are represented in **Table 7**.

Table 7. Effect of different KP-Cryst-Sp incubation times on spore capture.

[Sp]$_i$ (CFU.mL^{-1})	KP-Cryst-Sp (min)	Captured (CFU.mL^{-1})
8-Log	20	$4.21x10^4 \pm 1.64x10^3$
	90	$8.31x10^5 \pm 2.46x10^4$

It was observed that 90 min of incubation led to higher captured comparatively to 20 min.

Overall, in all these experiments a low spore capture was observed. At least 1.7-Log reduction was observed, from an initial concentration of 8-Log.

b) KP-Cryst concentration of 0.4 mg.mL^{-1}

Considering the positive effect on spore capture provided by KP-Cryst at 0.2 mg.mL^{-1}, we chose to further increase its concentration - 0.4 mg.mL^{-1} - on the MB surface. Moreover, spores unbound to MB-KP-Cryst were also plated for CFU count. **Table 8** shows the obtained data.

Table 8. Effect of different KP-Cryst concentration on spore capture.

$[Sp]_i$ (CFU.mL^{-1})	KP-Cryst (mg.mL^{-1})	Captured (CFU.mL^{-1})	Not captured (CFU.mL^{-1})
8-Log	0.2	$3.09x\ 10^6 \pm 4.57x10^4$	$7.90x10^7 \pm 2.45x10^6$
	0.4	$8.02\ x10^6 \pm 1.27x10^5$	$4.11x\ 10^6 \pm 1.57x10^5$

Results showed that higher spore captured was obtained with higher KP-Cryst concentration, 0.4 mg.mL^{-1}, being spore loss of 1.2-Log. This concentration was used in the subsequent assays. It was also observed that the sum of captured and not captured spores was lower than $[Sp]_i$ ($8.07x10^6 + 4.11x10^6 < 8.00x10^8$ CFU.mL^{-1}).

b.1.) Spore capture with lower $[Sp]_i$

The ability of MB-KP-Cryst to capture spores with [Sp]i = 5-Log was analysed through CFU count (**Table 9**).

Table 9. Performance of MB-KP-Cryst-Sp system on spore capture for $[Sp]_i$ = 5-Log

$[Sp]_i$ (CFU.mL^{-1})	KP-Cryst (mg.mL^{-1})	Captured (CFU.mL^{-1})	Not captured (CFU.mL^{-1})
5-Log	0.4	0.00	$4.45x10^4 \pm 2.33x10^3$

Remarkably, with an initial concentration of 5-Log spores, none was subsequently captured by MB-KP-Cryst, suggesting that the KP-Cryst-spores interaction could have been favoured by the pressure of spore concentration. Moreover, similarly to above, the sum of captured and not captured was lower than $[Sp]_i$: $0.00 + 4.45x10^4 < 5.00x10^5$ CFU.mL^{-1}.

3.5.3. Effect of pH

a) Evaluation of KP-Cryst-Sp binding with pH

The DLS analysis of a pure spore suspension ($1x10^6$ CFU.mL^{-1}) revealed a negative surface charge, of -19.1 ± 0.5 mV. Knowing that 7.13 is the isoelectric point of KP-Cryst, the effect of lowering pH on KP-Cryst-spores binding was evaluated, for two distinct [Sp]i: 5-Log and 7-Log. For that, 0.4 mg.mL^{-1} of KP-Cryst positively charged (suspended in buffer B, pH 5) was used, and the efficiency of the coating was determined by quantification of the UP (**Table 10**).

Table 10. Evaluation of spore coating by KP-Cryst at different $[Sp]_i$ (7-Log and 5-Log) with positively charged protein. Data analysed by *t-test*.****p-value < 0.0001 indicates significant statistical differences.

$[Sp]_i$ (CFU.mL^{-1})	KP-Cryst (mg.mL^{-1})	Efficiency (%)	Statistical differences
7-Log	0.4	68.40 ± 1.50	Yes (p-value < 0.0001)
5-Log		80.72 ± 1.79	

Looking at the table, the coating was significantly (p-value < 0.0001) more efficient when lower spores ($[Sp]_i$=5-Log) were in suspension.

To support this result, an analysis of the fluorescence intensity of KP-Cryst-Sp binding at two different pH's was performed through confocal microscopy. A volume corresponding to 0.4 mg.mL^{-1} of the protein, either suspended in buffer B (positively charged) or buffer A (neutral) was incubated with a pellet of concentrated spores initially at 7-Log. The results are illustrated in **Figure 15**.

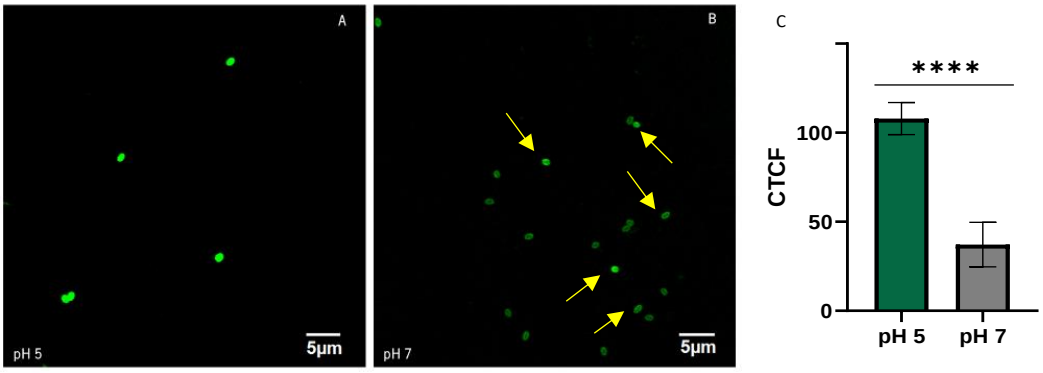

Figure 15. Confocal analysis of the *P. larvae* spores decorated with KP-Cryst at different pH. (A) KP-Cryst-spores at pH 5 (protein with a positive surface charge); (B) KP-Cryst-spores at pH 7 (protein neutral). (C) CTCF of spores incubated with KP-Cryst at pH 5 (positively charged) and pH 7 (neutral). Each bar represents the mean of 5 measurements (all spores for pH 5 and indicated by yellow arrow for pH 7) and the respective standard deviation. Data analysed by *t-test:* **** p-value < 0.0001 indicating statistical differences. CTCF = Integrated Density – (Area of selected cell X Mean fluorescence of background readings).

Although green-decorated spores were observed for both conditions, the analysis revealed a stronger CFTF occurring for KP-Cryst-Spores incubated at pH 5. While the former enabled a CTCF of 108, this value was significantly lower (37) when incubation occurred at pH 7. In subsequent tests, positively charged KP-Cryst was always used.

b) Effect of pH agitation on spore capture by MB-KP-Cryst-Sp

The ability of MB-KP-Cryst to capture spores with two distinct $[Sp]_i$ was analysed through BCA kit. For this, 5-Log and 7-Log spores were both resuspended in buffer B (pH 5) and added to the system. Additionally, KP-Cryst recovery by MB (theoretically corresponding to the percentage of protein initially placed that was captured) was also performed through BCA. The data obtained are presented in **Table 11**.

Table 11. Performance of MB-KP-Cryst-Sp system on spore recovery at pH 5.

$[Sp]_i$ ($CFU.mL^{-1}$)	KP-Cryst recovery by MB (%)	Captured ($CFU.mL^{-1}$)	Not captured ($CFU.mL^{-1}$)
7-Log	~99	$6.96x10^5 \pm 9.93x10^3$	$4.02x10^6 \pm 1.49x10^5$
5-Log		0.00	$5.21x10^4 \pm 1.12x10^3$

By analysing the table is possible to see that, despite almost 99 % KP-Cryst was coating MB , there was a reduction of 1.3-Log for $[Sp]_i$=7-Log, and an absence of recovery for $[Sp]_i$ = 5-Log. This latter result was similar for both pH tested.

Following this, agitation was increased in the MB-KP-Cryst-Sp incubation. Still, this did not alter spore capture when $[Sp]_i$ of 7-Log or 5-Log were used (data not shown).

b.1.) Effect of HBG on spore capture

In order to evaluate spore capture through artificially contaminated filtered HBG, the latter was equally mixed with $[Sp]_i$ of 7-Log and incubated with MB-KP-Cryst (using $1.5x10^5$ beads, KP-Cryst at 0.4 $mg.mL^{-1}$, 1 h 30 min incubation of MB-KP-Cryst-Sp). In comparison to the spore capture without HBG ($6.96x10^5 \pm 9.93x10^3$ $CFU.mL^{-1}$), it was possible to note that HBG presence result in a lower spore recovery ($1.0x10^5 \pm 1.35x10^4$ $CFU.mL^{-1}$).

3.5.4. Optimizing spore recovery from the low-concentrated suspensions

The focus of the next assays was on optimizing the capture for $[Sp]_i$ = 5-Log. The latter spore concentration is closer to what occurs in real infections; therefore, an efficient capture is critical for field applications.

First of all, we decided to completely saturate the MB with KP-Cryst to potentiate more successful interactions between the spores and the functionalized MB.

For that, three different concentrations of KP-Cryst were tested: 0.50, 0.75 and 0.90 $mg.mL^{-1}$ using $1.67x10^5$ MB. **Figure 16** shows the mean percentage of protein captured by MB, determined through the BCA kit.

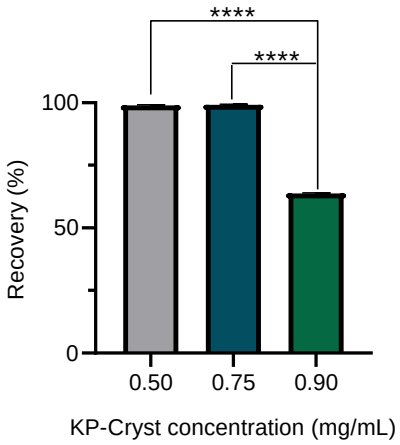

Figure 16. Peptide recovery by MB for different KP-Cryst concentrations (assays with the $1.67x10^5$ MB). Each value represents the mean and respective standard deviation of three replicates. Data analysed by *One-Way ANOVA*.****p-value < 0.0001 indicates significant statistical differences.

It was observed that up to 99 % of the protein was recovered by MB when 0.50 or 0.75 $mg.mL^{-1}$ were added. The recovery was significantly lower (p-value < 0.0001) for 0.9 $mg.mL^{-1}$ (~ 64 %). **Table 12** compares the theoretical (based on technical data sheet) and the real MB saturation (based on our experiments).

Table 12. Comparison among theoretical and real MB saturation for different KP-Cryst concentrations.

KP-Cryst ($mg.mL^{-1}$)	N° of MB	Theoretical MB saturation (%)	Real MB saturation (%)
0.50	1.67×10^5	62.5	~62.5
0.75		93.8	~93.8
0.90		100.0	~64.0

In the two lower concentrations of KP-Cryst, the theoretical MB saturation was similar to the experimental one. In contrast, for 0.9 $mg.mL^{-1}$, a 100 % saturation of the MB was expected (an excess of protein was added), but this was not verified. The MB deposition could be a possible explanation. Hence, in the next tests MB were ~94 % saturated. The MB higher efficiency of coating (comparatively to previous results reported in **Figure 9**) was confirmed by FOM (**Figure 17**).

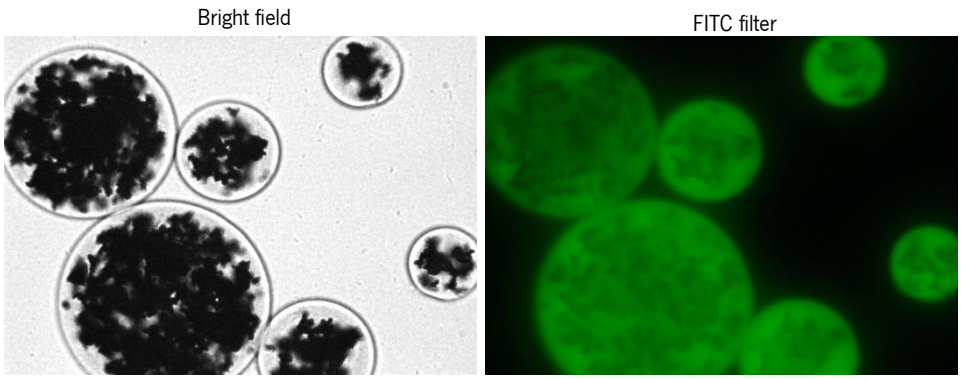

Figure 17. MB-KP-Cryst complex green-decorated (KP-Cryst at 0.75 mg.mL^{-1}). Image obtained for an exposition time of 50 ms.

a) Effect of different ratio MB-KP-Cryst : Sp on spore capture

Different ratios MB-KP-Cryst : Sp were tested in order to understand the influence of this factor on the spore capture by the system when initially 5-Log spores were used: different proportions could lead to different interactions between the spores and the functionalized MB.

Three different ratios were evaluated: 0.9, 10 and 20. In each assay, for the same number of MB, different spore concentration (CFU.mL^{-1})was added. The concentration of KP-Cryst used was 0.75 mg.mL^{-1} (MB saturation of ~94 %). The performance of MB-KP-Cryst-Sp system for each assay is shown in **Table 13**.

Table 13. Performance of MB-KP-Cryst-Sp system on spore capture for $[Sp]_i$ of 5-Log with different ratios MB-KP-Cryst : Sp.

$[Sp]_i$ (CFU.mL^{-1})	KP-Cryst recovery by MB (%)	MB-KP-Cryst : Sp	Captured (CFU.mL^{-1})	Not captured (CFU.mL^{-1})
5-Log	~99	0.9	$6.31x10^4 \pm 1.42x10^3$	$1.10x10^5 \pm 2.77x10^4$
		10	$4.06x10^4 \pm 1.88x10^3$	$1.55x10^4 \pm 1.91x10^3$
		20	$2.77x10^3 \pm 2.05x10^2$	$7.62x10^4 \pm 1.18x10^3$

It was noted an increased spore capture with smaller ratio MB-KP-Cryst : Sp. In fact, the ratio that allowed a higher spore recovery was 0.9, the lowest one.

It was further observed that the sum of captured and uncaptured spores was not always equal to $[Sp]_i$. MB-KP-Cryst : Sp = 0.9: $6.31x10^4$ CFU.mL^{-1} + $1.10x10^5$ CFU.mL^{-1} ~ 5-Log; MB-KP-Cryst : Sp =10: $4.06x10^4$ CFU.mL^{-1} + $1.55x10^4$ CFU.mL^{-1} < 5-Log; MB-KP-Cryst : Sp = 20: $2.77x10^3$ CFU.mL^{-1} + $7.62x10^4$ CFU.mL^{-1} < 5-Log.

Following this, **Table 14** summarizes the conditions that allowed the system to reach the initially proposed goal for spore loss (losses lower than 1-Log) starting from an initial spore concentration of 5-Log.

Table 14. Conditions that allowed the MB-KP-Cryst-Sp system to obtain a spore loss inferior to 1-Log starting from an initial spore concentration of 5-Log.

$[Sp]_i$ (CFU.mL^{-1})	KP-Cryst pH	MB (%)	MB-KP-Cryst	MB-KP-Cryst	MB-KP-Cryst : Sp
5-Log	5	~94.0	4 °C with 50 rpm	rt with 50 rpm	0.9 or 10.0

3.6. Spore detection from artificially infested samples using the complete MB-KP-Cryst-Sp-CBD procedure

Spore capture and detection by the MB-KP-Cryst-Sp-CBD system was analysed both in the presence and absence of filtered HBG, with 4h of incubation with germinants, and starting from 7-Log spores (since detection limit of optical microscope is 10^5 CFU.mL^{-1}). However, with this germination time, it was not possible to observe green-decorated cells in the FOM field when HBG was present. Thus, in this case, incubation period was then increased from 4 to 8 h and a positive result was observed. **Figure 18** shows the results of *P. larvae* cells detection through CBD for both assays.

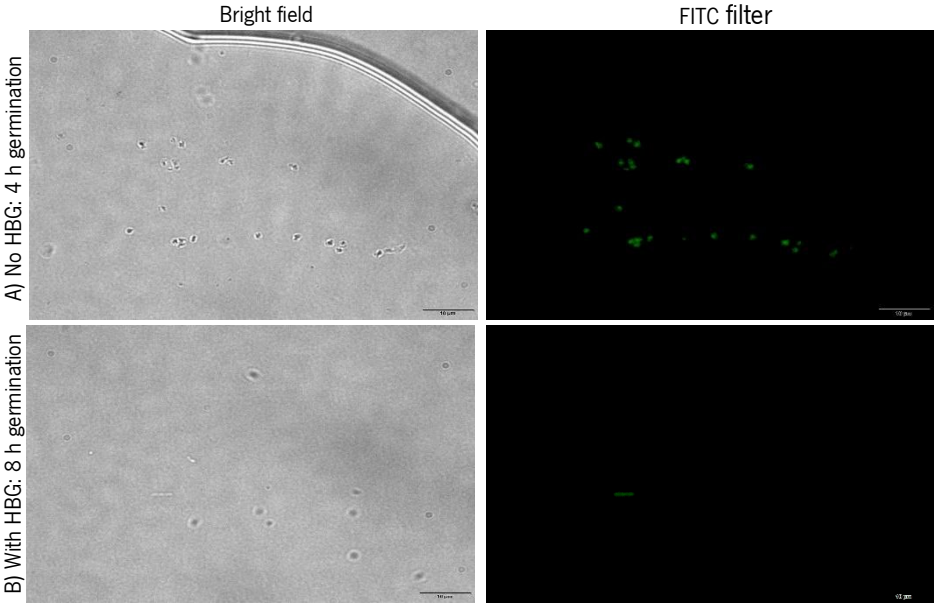

Figure 18. *P. larvae* germinated spores decorated with CBD (1000x magnification). (A) 4 h germination: CBD with germinative spores (MB-KP-Cryst-Sp-CBD system in the absence of HBG); (B) 8 h germination: CBD with germinative spores (MB-KP-Cryst-Sp-CBD system in the presence of HBG). Images obtained with 400 ms and 900 ms, respectively.

While, as observed previously (**Figure 8**), for 4h germination in HBG absence, green-decorated spores were clearly visible, for 8h, simulating real samples, a few green cells appeared. Moreover, for the latter, although spores appear in the microscope field, they apparently have not germinated.

Chapter 4. Discussion

Discussion

AFB is the deadliest bee larvae bacterial disease ever reported[2,6]. Taking into account the problems of existing methodologies for identifying *P. larvae*[60,69] and that the symptoms of AFB are only evident after the outbreak of the disease[2], monitoring the spore load in adult bees is extremely important since it reflects the current health status of the brood[2,26,65]. One of the critical steps in the detection of microbial pathogens is to obtain a detectable number of target cells[68]. In the specific case of *P. larvae*, the concentration of spores present in field samples (bees, honey, wax, etc.) will largely influence the limit of detection of a method. Taking this into account, in this work we tested the use of magnetic beads functionalised with a protein capable of binding to hair keratin (KP-Cryst) to purify and concentrate *P. larvae* spores previously to spore detection trough PlyPl23 CBD.

We have firstly evaluated the CBD ability to detect *P. larvae* dormant and germinating spores. As expected, the observation of green-decorated spores by FOM were not observed for dormant ones (**Figure 8.A**). In this case, the binding might have been prevented by the proteinaceous outer spore coat that hides, together with the outer cortex, the germ cell wall that resembles the vegetative PG[54].

Opposingly, spores germinated for at least 4 h were bright-green under FOM indicating that although not yet a complete mature PG from a vegetative cell, it allowed the CBD binding (**Figure 8.B**). This might have been possible due to the spore coat and outer membrane partial removal or disruption by DTT[70] and proteinase K[29]. While the first disrupted the disulphide bonds of spore coat, the second digested the peptide linkages[29]. Subsequently, coat permeability could have been increased towards lysozyme, which as a muramidase[29], promoting cortex hydrolysis and triggering germination through Ca^{2+}-DPA release[29,53,71]. The incubation with MYPGP supplemented with germinants - uric acid and L-tyrosine - reported as enhancing *P. larvae* spore germination[19] – should have accelerated the process.

Remarkably, we observed that (i) fluorescent intensity is lower in germinating spores when compared to bacterial cells and that (ii) not every germinating spores exhibited the same fluorescent intensity (**Figure 8.B and 8.C**). In the first case, results can be justified by an early stage of PG maturation with lower affinity to the peptide or/and by a lower number of available CBD receptors occurring in early germinating spores comparatively to vegetative cells[14]. In the second case, not all the spores should have been in identical germinative state 4 h after triggering germination[72].

We have then tested the efficacy of functionalizing MB with KP-Cryst protein. The FITC labelling allowed to confirm the coating through FOM when bright green MB were observed, but curiously, it seemed that the protein distribution was not homogenous along the bead surface (**Figure 9.B**). This might have been caused by (a) a low concentration of protein added per MB or by (b) a fast deposition of MB when preparing the coating, impairing the exposure of the total surface to the protein. In several studies where similar beads were used, high sedimentation rates were observed, and consequently the bead coating was always performed under stirring[68,73]. Based on that, subsequent incubations involving MB occurred with agitation.

Considering our aim of using MB-KP-Cryst to capture spores from field samples, the specificity of the protein for spores was evaluated.

Firstly, there was no apparent binding between the particles from HBG and MB-KP-Cryst – the observed signal was due to tissues autofluorescence[74] (**Figure 10.A**). Nevertheless, the observation of *P. larvae* green-decorated cells (**Figure 10.B**) indicated that, if the protein binds to vegetative cells, it will possibly bind to bee commensal bacteria[75]. These might compete directly with spores, thereby reducing the available binding area of MB and compromising the effectiveness of spore capture.

In an attempt to overcome this problem, we've tested the effect of pre-heating these samples. Whereas pre-heating of the *P. larvae* cells at 80 °C failed to prevent KP-Cryst- vegetative cell binding (**Figure 11.A**), no protein attachment was detected when cells pre-treated at 95 °C (**Figure 11.B**). As such, this may be a procedure to be tested in further assays to prevent non-specific binding of the protein.

After setting conditions to obtain MB coating with KP-Cryst, the KP-Cryst-Sp binding was optimized. Firstly, the shortest time that provides an effective spore capture by KP-Cryst was tested using several incubation times. The incubations of 20, 25 and 30 min allowed to see green-decorated spores with an exposure time of 200 ms, contrary to what happened for 10 and 15 min, where this was only possible with 400 ms. Therefore, subsequent incubations were performed for 20 min.

Then, the interference of the sample matrix in the KP-Cryst-Sp binding was evaluated. This can be a critical feature when looking at a field application. The influence of the matrix on the attachment of the ligand to its receptor, hindering the detection/collection of the target microorganism have been often reported[76–78]. Results revealed the interference of HBG in KP-Cryst-Sp binding showing no bright-green spores by FOM after incubation in such a matrix (**Figure 13**). A different result was obtained when HBG was filtered through 0.45 μm - previously to spore artificial contamination: green-decorated spores were

visualized (**Figure 14**), however the observation required higher fluorescent exposition time comparatively to spores in water (1000 and 200 ms, respectively). This suggests a still negative influence of some compounds dissolved in HBG on KP-Cryst-Sp binding, confirmed with MB-KP-Cryst-Sp binding in HBG (spore loss of 3.4-Log). However, and unexpectedly, similar spore loss was obtained (3-Log) replacing HBG by water (**Table 5**), suggesting that besides the HBG effect other variables were affecting KP-Cryst-Sp binding. Simultaneously, the ability of the used decoating agents to dissociate spores from MB-KP-Cryst was proved, as 90 % of the spores were released from the MB (**Table 5**).

In order to improve the capture of spores by the system, the protein concentration on the MB surface was increased from 0.07 to 0.20 mg.mL^{-1}, resulting in a higher spore capture efficacy: from 3.0 x 10^5 to 8.3 x 10^5 CFU.mL^{-1} (**Table 6**). KP-Cryst should have become more available for spore binding in MB surface. On the other hand, as in several studies the most suitable temperature for the purification of recombinant His-tag proteins is 4°C[79–81], the latter was introduced in MB-KP-Cryst incubation aiming to promote a better interaction between the MB and the protein. This consequently led to an improved spore capture and spore loss decreased from 2.2-Log to 1.7-Log. Based on this, MB was further incubated with KP-Cryst at 4 °C.

Although the loss of spores was still higher than 1-Log (defined as reasonable in our initial aim: spore loss similar to that obtained by HistoDenz® gradient), we tried to decrease the total process time already at this stage. So, the MB-KP-Cryst-Sp incubation was reduced from 1 h 30 min to 20 min (previously defined as optimal for KP-Cryst-Sp binding) (**Table 7**). The observed high spore loss - 3.5-Log - suggested that this was not sufficient to obtain an efficient MB-KP-Cryst interactions with spores[73], and then we went back to the incubation time of 1h 30 min.

Assuming that increasing KP-Cryst concentration on MB surface would make it more available and lead to greater spore capture, 0.4 mg.mL^{-1} were used when preparing MB-KP-Cryst. Not only an increase in capture was observed, but the loss of spores was now closer to 1-Log (1.2-Log, specifically) (**Table 8**). Nevertheless, it is important to refer that the sum of captured spores and unbound spores was inferior to the $[Sp]_i$ (8-Log), indicating that not all spores germinated from MB or some loss of spores may have occurred during the samples processing.

We've decided then to test these new settings with an initial lower spore concentration, in order to mimic field conditions, and 5-Log spores were used. However, unexpectedly, no spores were recovered by the system (**Table 9**). This suggested that, if a greater concentration of spores is needed to enable KP-

Cryst-Sp binding is because some repulsive forces are interacting in the capture. Such event might have been attenuated by the pressure of high concentrations (results obtained with $[Sp]_i$= 8-Log).

Based on this assumption, a closer look at KP-Cryst electrical charge revealed an isoelectric point of 7.13[67], which means neutrality at pH 7[82,83] - pH of the storage buffer. On the other hand, the analysis by DLS revealed that the spore surface was negatively charged (zeta potential of -19.1 mV). Accordingly, we hypothesized that lowering KP-Cryst buffer to pH 5 could make the protein positively charged, promoting attraction forces with the oppositely charged spores[83–85]. This was confirmed firstly by protein quantification (**Table 10**) and later by Confocal microscopy (**Figure 15**). After incubating KP-Cryst with 5-Log spores, less concentration of unbound protein was detected compared to 7-Log, suggesting a higher coating efficiency even with a lower spore concentration. Accordingly, a higher fluorescence intensity was observed in KP-Cryst-Sp binding at pH 5 instead pH 7. Consequently, we decided to use positively charged KP-Cryst (pH 5 buffer) in all the further spore capture assays. Considering that the pH of HBG ranges between 5.5 and 6.0, the use of that pH would even be easier to mimic in real samples.

Surprisingly, lowering reaction buffer pH did not improve spore capture by MB-KP-Cryst neither using high or low initial concentrations of spores: there was a loss of more than 1-Log for $[Sp]_i$ = 7-Log and no capture for 5-Log – **Table 11**. In both cases, MB captured all KP-Cryst (~99% - determined by protein quantification) and therefore this was not the limiting factor. This could have happened due to the deposition of MB which made KP-Cryst less available for spores[73]. It seemed that interactions between functionalized MB and spores are critical for the capture[73]. In an attempt to overcome this issue, we have increased stirring in the MB-KP-Cryst-Sp incubation trying to improve MB dispersion, and consequently enhance the opportunity for interacting with spores. Nonetheless, no improvements were observed and spore loss were in 1.3-Log of magnitude. Thus, in this situation, perhaps the increase of sample volume could have provided a better dispersion of the MB.

Even with losses higher than 1-Log, foreseeing spore detection from field samples we have tested again the effect of HBG on spore capture using $[Sp]_i$ of 7-Log. Despite the expected lower MB-KP-Cryst-Sp binding efficacy (spore loss was 2-Log), comparably to the first assay using HBG (spore loss of 3.4-Log using 0.07 $mg.mL^{-1}$ of KP-Cryst), can be said that the increase in KP-Cryst concentration, was probably the factor that caused a smaller loss of the system – since, as already mentioned, HBG pH is in the range 5.5 - 6.0.

Overall, we observed a spore loss of 1.2-Log (slightly superior to defined in our objective) when higher initial spore concentrations were used was and that HBG negatively affects the interaction between protein

and spores. In addition, there was an impossibility of capturing spores from $[Sp]_i$ = 5-Log which could hinder the feasibility of the method. So, the focus was then to optimize the capture from low-concentrated suspensions.

Considering that the frequency of interactions between the functionalised MB and spores is lower with $[Sp]_i$ = 5-Log comparatively to 7-Log, we've decided, first, to (i) saturate all MB surface by KP-Cryst and, subsequently, (ii) vary the ratio MB-KP-Cryst : Sp. Regarding (i), a MB saturation of 94 % was determined by protein quantification (**Figure 16**) and, then, confirmed by FOM (**Figure 17**). Indeed, MB were practically all green over their entire surface, which could increase the successful interactions between MB-KP-Cryst and spores as a wider area is available for spore binding. So, we decided to use 94 % of MB saturation in the MB-KP-Cryst-Sp system's with different ratios MB-KP-Cryst : Sp. It is important to refer that after MB functionalization, the quantification of UP revealed that 99 % of KP-Cryst has been captured by MB, confirming the expected MB saturation. Concerning (ii), the evaluation of system efficacy revealed that spore capture was improved the lower MB-KP-Cryst : Sp was (**Table 13**). Moreover, the ratios of 1 and 10 both allowed a spore loss inferior to 1-Log (0.4 and 0.6-Log, respectively). In fact, the recovery of about 60 % of the spores was similar to that obtained by Loessner et al. (2007)[68], with 10^5 *Listeria* cells using similar beads. So, the achievement of the initially proposed goal may have derived from the concerted action of factors (i) and (ii): the nearly entire MB surface covered with KP-Cryst associated with the proportions of 1 or 10 probable improved interaction between MB-KP-Cryst and spores in the solution (**Table 14**).

Lastly, as expected, the comparison between the detection efficacy of *P. larvae* spores from pure suspensions (spores in buffer B) and from real samples (spores in HBG) revealed differences. While in the first case, the observation of several green-decorated spores (6 per field, in average) by FOM (Figure 14) indicated that the implemented system allowed to detect spores from a 7-Log concentrated suspension with 4 h germination; in the second case, although present in the microscopic field, very few spores were green-decorated and only after 8 h of germination. Spores might have been captured (MB-KP-Cryst efficient binding), but most of them seem not to have germinated (**Figure 18**). So, it is possible to infer that HBG delay germination and that germination process must be optimized in order to allow a faster detection. Indeed, Alvarado and colleagues (2013)[19] demonstrated that phenolic compounds, such as polyphenols and indoles, usually presents in bee feeding, namely royal jelly[86,87], could inhibit *P. larvae* spore germination.

Here it has been demonstrated that magnetic beads functionalised with KP-Cryst (His-tagged) fusion protein are suitable for capturing *P. larvae* spores by KP-Cryst ability to bind to keratin-like proteins[67], present in the spore coat of *P. larvae*. In addition, PlyPl23 CBD has also been proven to be able to bind to germinating spores, allowing its detection under fluorescence microscopy through GFP.

The detection of spores from water lasts for less than 24 h, an important result encouraging the development of a fast detection kit. However, the same was not verified on HBG, making low efficacy of spore germination in real samples our main concern.

Chapter 5.
Conclusions & Future perspectives

5.1. Conclusion

The capture and subsequent, detection of *P. larvae* spores was successfully achieved through the MB-KP-Cryst-Sp-CBD system.

Previous works has shown that HistoDenz® gradient allows to recover and purify spores, although it implies a loss of approximately 1-Log. After several optimizations, our system proved to be advantageous.

We were able to present a totally new protocol with a similar efficiency in spore recovery, but with less centrifugation steps. This is a mandatory requirement for an *on-site* test. In addition, the whole procedure can be completed on a working day, an important result foreseeing a fast detection kit.

However, some concerns have been raised when its application was designed in field samples. Although spore capture could be confirmed in artificially infected bees, longer germination time and also more efficient germination are needed to enable detection by CBD. Additional optimizations are required to improve germination in such conditions.

Still, the margin to reduce the operating time of the protocol, for example by providing MB previously functionalised in the kit, and to reduce the centrifugation steps still existing using magnetic beads are encouraging insights that supports the development of a fast AFB control kit to use in hives.

5.2. Future Perspectives

Despite the promising results, more studies should be done for a higher efficiency of the MB-KP-Cryst-Sp-CBD system. For example, other studies could be conducted with other types of beads, more homogeneous and with a better dispersion[67]. Another alternative could be to plan hydrodynamic studies to optimize conditions that allows to have beads in suspension since, after slight agitation, the beads sediment[69].

Novel strategies of treating bee samples must be developed in order to improve KP-Cryst-Sp binding in HBG. For example: (i) combining a pre-heat treatment with a filtration through > 1 μm or (ii) using a filter grinding bag to crush bees and recover the resulting fluids to proceed with the protocol.

In addition, it is necessary to improve the use of this system to capture low concentrated spores from field samples. Besides optimizing the MB-KP-Cryst capture efficiency, it might be needed to increase the sample size to increase the detection limit.

In order to reduce the total running time of the protocol, MB should be pre-functionalised with KP-Cryst. Also concerning time saving, other incubation times of MB-KP-Cryst-Sp may be tested, with different stirrings, saturation of MB, and even the use of other types of shakers (rotative or obliquus). Moreover, for the germination improvement in real samples, the use of germinating-specific enzymes such as SleB and CwlJ might be an option.

The complete absence of centrifugation steps in the protocol can be obtained through the functionalization of MB with CBD, which can allow magnetic capture of germinated spores after binding occurs.

Increasing the sensitivity of the detection method is also in perspective, envisaging on-site use. For that, reporter probes such as Horseradish peroxidase can be experimented, which can be detectable by highly sensitive Chemiluminescence technology, preventing the use of FOM.

Finally, the system efficiency must be validated in field studies, using samples randomly collected from hives.

Bibliography

1. Kritsky, G. Beekeeping from antiquity through the middle ages. *Annual Review of Entomology*, **62**, 249-264 (2017). doi:10.1146/annurev-ento-031616-035115

2. Stephan, J. G., Miranda, J. R. De & Forsgren, E. Correction to : American foulbrood in a honeybee colony : spore - symptom relationship and feedbacks between disease and colony development. *BMC Ecol.* **20**, 1-14 (2020). doi:10.1186/s12898-020-00285-8

3. Genersch, E. American Foulbrood in honeybees and its causative agent, *Paenibacillus larvae*. J*ournal of invertebrate pathology*, **103**, S10-S19 (2010). https://doi.org/10.1016/j.jip.2009.06.015

4. Greenleaf, S. S., & Kremen, C. Wild bees enhance honey bees' pollination of hybrid sunflower. *Proceedings of the National Academy of Sciences*, **103**, 13890-13895 (2006). https://doi.org/10.1073/pnas.0600929103

5. Fünfhaus, A., Göbel, J., Ebeling, J. & Genersch, E. Swarming motility and biofilm formation of *Paenibacillus larvae*, the etiological agent of American Foulbrood of honeybees (Apis mellifera). *Scientific reports*, **8**, 1-12 (2018). doi:10.1038/s41598-018-27193-8

6. Genersch, E. Foulbrood diseases of honey bees—from Science to Practice. *In Beekeeping–From Science to Practice* 157-174 (Springer, 2017). doi:10.1007/978-3-319-60637-8

7. Neal, S. T. O., Anderson, T. D. & Wu-smart, J. Y. ScienceDirect Interactions between pesticides and pathogen susceptibility in honey bees. *Curr. Opin. Insect Sci.* **26**, 57-62 (2018). doi:10.1016/j.cois.2018.01.006

8. Congressional Research Servicec. *Bee Health : Background and Issues for Congress*. (2015).

9. Garcia-Gonzalez, E. & Genersch, E. Honey bee larval peritrophic matrix degradation during infection with Paenibacillus larvae, the aetiological agent of American foulbrood of honey bees, is a key step in pathogenesis. *Environ. Microbiol.* **15**, 2894–2901 (2013). https://doi.org/10.1111/1462-2920.12167

10. Mahdi, O. S. & Fisher, N. A. Sporulation and germination of *Paenibacillus larvae* cells. *Curr. Protoc. Microbiol.* **48**, 9E.2.1-9E.2.10 (2018). https://doi.org/10.1002/cpmc.46

11. Arbia, A., & Babbay, B. Management strategies of honey bee diseases. *Journal of Entomology*, **8**, 1-15. (2011). http://dx.doi.org/10.3923/je.2011.1.15

12. Alvarado, I., Margotta, J. W., Aoki, M. M., & Abel-Santos, E. (2017). Inhibitory effect of indole analogs against *Paenibacillus larvae*, the causal agent of American foulbrood disease. *Journal of Insect Science*, **17**, (2017). https://doi.org/10.1093/jisesa/iex080

13. Knispel, H., Hertlein, G., Fünfhaus, A., & Ebeling, J. Biology of *Paenibacillus larvae*, a deadly pathogen of honey bee larvae. *Appl. Microbiol. Biotechnol.* **100**, 7387–7395 (2016).

14. Santos, S. B., Oliveira, A., Melo, L. D. R. & Azeredo, J. Identification of the first endolysin Cell Binding Domain (CBD) targeting *Paenibacillus larvae*. *Sci. Rep.* **9**, 1–9 (2019). https://doi.org/10.1038/s41598-019-39097-2

15. Forsgren, E., Stevanovic, J. & Fries, I. Variability in germination and in temperature and storage resistance among *Paenibacillus larvae* genotypes. *Vet. Microbiol.* **129**, 342–349 (2008). https://doi.org/10.1016/j.vetmic.2007.12.001

16. Alippi, A. M. A comparison of laboratory techniques for the detection of significant bacteria of the honey bee, *Apis mellifera*, in Argentina. *Journal of Apicultural Research*, **30**, 75-80 (1991). https://doi.org/10.1080/00218839.1991.11101237

17. Genersch, E., Forsgren, E., Pentikäinen, J. & Fries, I. Reclassification of *Paenibacillus larvae subsp. pulvifaciens* and *Paenibacillus larvae subsp. larvae* as *Paenibacillus larvae* without subspecies differentiation. *International Journal of Systematic and Evolutionary Microbiology*, **56**, 501-511 (2006). https://doi.org/10.1099/ijs.0.63928-0

18. Oliveira, A., Melo, L. D., Kropinski, A. M., & Azeredo, J. Complete genome sequence of the broad-host-range *Paenibacillus larvae* phage phiIBB_Pl23. *Genome announcements*, **1**, 2–3 (2013). DOI: 10.1128/genomeA.00438-13

19. Alvarado, I., Phui, A., Elekonich, M. M. & Abel-Santos, E. Requirements for In vitro germination of *Paenibacillus larvae* spores. *J. Bacteriol.* **195**, 1005–1011 (2013). DOI: 10.1128/JB.01958-12

20. Locke, B., Low, M. & Forsgren, E. An integrated management strategy to prevent outbreaks and eliminate infection pressure of American foulbrood disease in a commercial beekeeping operation. *Prev. Vet. Med.* **167**, 48–52 (2019). https://doi.org/10.1016/j.prevetmed.2019.03.023

21. Alippi, A. M., López, A. C., & Aguilar, O. M. Differentiation of *Paenibacillus larvae subsp. larvae*,

the cause of American foulbrood of honeybees, by using PCR and restriction fragment analysis of genes encoding 16S rRNA. *Applied and Environmental Microbiology*, **68**, 3655-3660 (2002). DOI: 10.1128/AEM.68.7.3655-3660.2002

22. Lamei, S., Stephan, J. G., Nilson, B. & Forsgren, E. Feeding honeybee colonies with honeybee-specific lactic acid bacteria (Hbs-LAB) does not affect colony-level Hbs-LAB composition or *Paenibacillus larvae* spore levels, although American Foulbrood affected colonies harbor a more diverse Hbs-LAB community. *Microbial ecology*, **79**, 743-755 (2020). https://doi.org/10.1007/s00248-019-01434-3

23. Beims, H., Bunk, B., Erler, S. & Steinert, M. Discovery of *Paenibacillus larvae* ERIC V: Phenotypic and genomic comparison to genotypes ERIC I-IV reveal different inventories of virulence factors which correlate with epidemiological prevalences of American Foulbrood. *International Journal of Medical Microbiology*, **310**, 151-394 (2020). doi:10.1016/j.ijmm.2020.151394

24. Ghorbani-Nezami, S., LeBlanc, L., Yost, D. G. & Jeanne, R. Phage therapy is effective in protecting honeybee larvae from American foulbrood disease. *J. Insect Sci.* **15**, 1–5 (2015). https://doi.org/10.1093/jisesa/iev051

25. Oliveira, A., Leite, M., Kluskens, L. D. & Azeredo, J. The first *Paenibacillus larvae* bacteriophage endolysin (PlyPl23) with high potential to control American foulbrood. *PLoS One*, **10**, e0132095 (2015). https://doi.org/10.1371/journal.pone.0132095

26. Gende, L., Satta, A., Ligios, V., & Floris, I. Searching for an American foulbrood early detection threshold by the determination of *Paenibacillus larvae* spore load in worker honey bees. *Bulletin of insectology*, **64**, 229-233 (2011).

27. Heyndrickx, M., Vandemeulebroecke, K., Hoste, B.& Berkeley, R. C. W. (1996). Reclassification of *Paenibacillus* (formerly *Bacillus*) *pulvifaciens* (Nakamura 1984) Ash et al. 1994, a later subjective synonym of *Paenibacillus* (formerly *Bacillus*) *larvae* (White 1906) Ash et al. 1994, as a subspecies of *P. larvae*, with emended descriptions of *P. larvae* as *P. larvae subsp. larvae* and *P. larvae subsp. pulvifaciens*. *International journal of systematic and evolutionary microbiology*, **46**, 270-279 (1996). https://doi.org/10.1099/00207713-46-1-270

28. Yue, D., Nordhoff, M., Wieler, L. H. & Genersch, E. Fluorescence in situ hybridization (FISH) analysis of the interactions between honeybee larvae and *Paenibacillus larvae*, the causative

agent of American foulbrood of honeybees (*Apis mellifera*). *Environ. Microbiol.* **10**, 1612–1620 (2008).

29. Mundra, R. V., Mehta, K. K., Wu, X., & Dordick, J. S. Enzyme-driven *Bacillus* spore coat degradation leading to spore killing. *Biotechnology and bioengineering*, **111**, 654-663 (2014). https://doi.org/10.1002/bit.25132

30. Ansari, M. J., Al-Ghamdi, A., Usmani, S. & Omer, M. In vitro evaluation of the effects of some plant essential oils on *Paenibacillus larvae*, the causative agent of American foulbrood. *Biotechnology & Biotechnological Equipment*, **30**, 49-55 (2016). https://doi.org/10.1080/13102818.2015.1086690

31. Fuselli, S. R., Gende, L. B., Rosa, S. B. G. & Fritz, R. Inhibition of *Paenibacillus larvae subsp larvae* by the essential oils of two wild plants and their emulsifying agents. *Spanish Journal of Agricultural Research*, **3**, 220–224 (2005).

32. Lopes, L. Q., Santos, C. G., de Almeida Vaucher, R., & Santos, R. C. Evaluation of antimicrobial activity of glycerol monolaurate nanocapsules against American foulbrood disease agent and toxicity on bees. *Microbial pathogenesis*, **97**, 183-188 (2016). https://doi.org/10.1016/j.micpath.2016.05.014

33. Antúnez, K., Harriet, J., Gende, L.. & Zunino, P. Efficacy of natural propolis extract in the control of American Foulbrood. *Veterinary microbiology*, **131**, 324–331 (2008). https://doi.org/10.1016/j.vetmic.2008.04.011

34. Mirgorodskaya, E., Bukovská, G., Gobom, J. & Šimúth, J. Towards functional proteomics of minority component of honeybee royal jelly: The effect of post-translational modifications on the antimicrobial activity of apalbumin2. *Proteomics*, **9**, 2131-2138. (2009). doi:10.1002/pmic.200800705

35. Powell, J. E., Martinson, V. G., Urban-Mead, K. & Moran, N. Routes of acquisition of the gut microbiota *Apis mellifera* of the honey bee. *Appl. Environ. Microbiol.* **80**, 7378–7387 (2014). DOI: 10.1128/AEM.01861-14

36. Evans, J. D. & Armstrong, T. Antagonistic interactions between honey bee bacterial symbionts and implications for disease. *BMC ecology,* **9**, 1–9 (2006). https://doi.org/10.1186/1472-6785-6-4

37. Jaouani, I., Abbassi, M. S., Alessandria, V.& Cocolin, L. High inhibition of *Paenibacillus larvae* and *Listeria monocytogenes* by *Enterococcus* isolated from different sources in Tunisia and identification of their bacteriocin genes. *Letters in applied microbiology*, **59**, 17-25 (2014). doi:10.1111/lam.12239

38. Hernández-López, J., Crockett, S., Kunert, O. & Riessberger-Gallé, U. *In vitro* growth inhibition by *Hypericum* extracts and isolated pure compounds of *Paenibacillus larvae*, a lethal disease affecting honeybees worldwide. *Chemistry & biodiversity*, **11**, 695-708 (2014). https://doi.org/10.1002/cbdv.201300399

39. Reyes, M. G., Torres, M. J., Maggi, M. D. & Audisio, M. C. *In vitro* inhibition of *Paenibacillus larvae* by different extracts and pure compounds from *Flourensia spp*. *Industrial crops and products*, **50**, 758-763 (2013). https://doi.org/10.1016/j.indcrop.2013.07.062

40. Fernández, N. J., Damiani, N., Podaza, E. A. & Gende, L. B. *Laurus nobilis L*. extracts against *Paenibacillus larvae*: Antimicrobial activity, antioxidant capacity, hygienic behavior and colony strength. *Saudi journal of biological sciences*, **26**, 906-912 (2019). doi:10.1016/j.sjbs.2018.04.008

41. Sidorov, V. A. I., Uczek, K. B., Egiet, A. S. & Ambrowski, G. Z. Activity of selected plant extracts against honey bee pathogen *Paenibacillus larvae*. *Apidologie,* **49**, 687–704 (2018). https://doi.org/10.1007/s13592-018-0586-y

42. Schmelcher, M. & Loessner, M. J. Application of bacteriophages for detection of foodborne pathogens. *Bacteriophage*, **4**, e28137 (2014).

43. Ribeiro, H. G., Melo, L. D., Oliveira, H. & Oliveira, A. Characterization of a new podovirus infecting *Paenibacillus larvae*. *Scientific reports*, **9**, 1-12 (2019). doi:10.1038/s41598-019-56699-y

44. Ribeiro, H. G., Correia, R., Moreira, T., Boas, D. V. & Azeredo, J. Bacteriophage biodistribution and infectivity from honeybee to bee larvae using a T7 phage model. *Scientifid Reports,* **9**,1–8 (2019). doi:10.1038/s41598-018-36432-x

45. Yost, D. G., Tsourkas, P. & Amy, P. S. Experimental bacteriophage treatment of honeybees (*Apis mellifera*) infected with *Paenibacillus larvae* , the causative agent of American Foulbrood Disease *Bacteriophage* **6**, 1–15 (2016). https://doi.org/10.1080/21597081.2015.1122698

46. LeBlanc, L., Nezami, S., Yost, D. & Amy, P. S. Isolation and characterization of a novel phage lysin active against *Paenibacillus larvae*, a honeybee pathogen. *Bacteriophage*, **5**, e1080787 (2015). https://doi.org/10.1080/21597081.2015.1080787

47. Grady, E. N., MacDonald, J., Liu, L.. & Yuan, Z. C. Current knowledge and perspectives of *Paenibacillus*: A review. *Microb. Cell Fact.* **15**, 1–18 (2016).

48. Rauch, S., Ashiralieva, A., Hedtke, K. & Genersch, E. Negative correlation between individual-insect-level virulence and colony-level virulence of *Paenibacillus larvae*, the etiological agent of american foulbrood of honeybees. *Appl. Environ. Microbiol.* **75**, 3344–3347 (2009). DOI: 10.1128/AEM.02839-08

49. OIE Terrestrial Manual.American Foulbrood of honeybees with *Paenibacillus larvae*. (2019).

50. Paredes-Sabja, D., Setlow, P. & Sarker, M. R. Germination of spores of *Bacillales* and *Clostridiales* species: Mechanisms and proteins involved. *Trends Microbiol.* **19**, 85–94 (2011). https://doi.org/10.1016/j.tim.2010.10.004

51. Mao, L., Jiang, S., Wang, B. & Chen, K. (2011). Protein profile of *Bacillus subtilis* spore. Current microbiology, **63**, 198–205 (2011). doi:10.1007/s00284-011-9967-4

52. Ross, C. & Abel-santos, E. The Ger Receptor Family from Sporulating Bacteria. *Curr. Issues Mol. Biol.*, **12**, 147–158 (2016). doi:10.21775/cimb.012.147

53. Arechiga, V. P. Relative Expression of Germination Genes SleB, GerAC, and gpr in Heat Treated Bacillus licheniformis and Bacillus subtilis. (California Polytechinique State University, San Luis Obispo, 2014).

54. Amon, J. D., Yadav, A. K., Ramirez-Guadiana, F. H. & Rudner, D. Z. SwsB and SafA are required for CwlJ-dependent spore germination in *Bacillus subtilis*. *Journal of bacteriology*, **202** (2020). doi:10.1128/JB.00668-19

55. Lai, E. M., Phadke, N. D., Kachman, M. T., & Driks, A. Proteomic analysis of the spore coats of *Bacillus subtilis* and *Bacillus anthracis*. *Journal of bacteriology*, **185**, 1443-1454. (2003).

56. Stephan, J. G., de Miranda, J. R., & Forsgren, E. (2020). American foulbrood in a honeybee colony: spore-symptom relationship and feedbacks. *BMC ecology*, **20**, 1-14 (2020). doi:10.1186/s12898-020-00283-w

57. Genersch, E., Ashiralieva, A., & Fries, I. Strain-and genotype-specific differences in virulence of *Paenibacillus larvae subsp. larvae*, a bacterial pathogen causing American foulbrood disease in honeybees. *Applied and Environmental Microbiology*, **71**, 7551-7555 (2005). DOI: 10.1128/AEM.71.11.7551-7555.2005

58. Neuendorf, S., Hedtke, K., Tangen, G., & Genersch, E. Biochemical characterization of different genotypes of Paenibacillus larvae subsp. larvae, a honey bee bacterial pathogen. *Microbiology*, **150**, 2381-2390. (2004). doi:10.1099/mic.0.27125-0

59. Yones, M. S., Ma'moun, S. A. M., Farag, R. M. A. & El-raouf, M. M. A. Hyperspectral application for early diagnosis of American foulbrood disease in the honeybee (*Apis mellifera L* .) *larvae*. *Egypt. J. Remote Sens. Sp. Sci.* **22**, 271–277 (2019). https://doi.org/10.1016/j.ejrs.2019.05.002

60. Crudele, S., Ricchiuti, L., Ruberto, A. & Rossi, F. Quantitative PCR (qPCR) vs culture-dependent detection to assess honey contamination by *Paenibacillus larvae*. *J. Apic. Res.* **59**, 218-222 (2019). https://doi.org/10.1080/00218839.2019.1689900

61. Rossi, F., Amadoro, C., Ruberto, A. & Ricchiuti, L. Evaluation of Quantitative PCR (qPCR) Paenibacillus larvae Targeted Assays and Definition of Optimal Conditions for Its Detection/Quantification in Honey and Hive Debris. *Insects* **9**, 165 (2018). https://doi.org/10.3390/insects9040165

62. Kwon, S. J., Kim, D., Lee, I. & Dordick, J. S. Sensitive multiplex detection of whole bacteria using self-assembled cell binding domain complexes. *Analytica chimica acta*, **1030**, 156-165 (2018). https://doi.org/10.1016/j.aca.2018.05.008

63. Wilson, I. G. Inhibition and facilitation of nucleic acid amplification. *Applied and environmental microbiology*, **63**, 3741–3751 (1997).

64. Saville, B. G. Differentiation of virulent and biological control Paenibacillus larvae strains associated with American foulbrood in bee hives (University of York, 2011)

65. Forsgren, E., & Laugen, A. T. Prognostic value of using bee and hive debris samples for the detection of American foulbrood disease in honey bee colonies. *Apidologie* **45**, 10–20 (2014). http://dx.doi.org/10.1007/s13592-013-0225-6

66. Alvarado, I., Elekonich, M. M., Abel-Santos, E. & Wing, H. J. Comparison of in vitro methods for

the production of *Paenibacillus larvae* endospores. *J. Microbiol. Methods* **116**, 30–32 (2015). https://doi.org/10.1016/j.mimet.2015.06.011

67. Tinoco, A., Gonçalves, J., Silva, C., & Ribeiro, A. Crystallin fusion proteins improve the thermal properties of hair. *Frontiers in bioengineering and biotechnology*, **7**, 1–12 (2019). https://doi.org/10.3389/fbioe.2019.00298

68. Kretzer, J. W., Lehmann, R., Schmelcher, M., & Loessner, M. J. (2007). Use of high-affinity cell wall-binding domains of bacteriophage endolysins for immobilization and separation of bacterial cells. *Applied and environmental microbiology*, **73**, 1992–2000 (2007). DOI: 10.1128/AEM.02402-06

69. Popiela, E., Owczarek, B. & Jo, E. Phages in Therapy and Prophylaxis of American Foulbrood – *Recent Implications From Practical Applications*, **11**, 1–16 (2020). https://doi.org/10.3389/fmicb.2020.01913

70. Kutima, P. M., & Foegeding, P. M. Involvement of the spore coat in germination of B*acillus cereus* T spores. *Applied and Environmental Microbiology*, **53**, 47-52 (1987).

71. Escobar-Cortés, K., Barra-Carrasco, J., & Paredes-Sabja, D. Proteases and sonication specifically remove the exosporium layer of spores of *Clostridium difficile* strain 630. *Journal of microbiological methods*, **93**, 25-31. (2013). https://doi.org/10.1016/j.mimet.2013.01.016

72. Moir, A., & Cooper, G. Spore germination. *The Bacterial Spore: From Molecules to Systems*, 217-236 (2016). https://doi.org/10.1128/9781555819323.ch11

73. Tu, S., Uknalis, J. & Ars, U. Factors FACTORS AFFECTING THE BACTERIAL CAPTURE EFFICIENCY OF IMMUNO BEADS : A COMPARISON BETWEEN BEADS WITH DIFFERENT SIZE AND DENSITY. J*ournal of Rapid Methods & Automation in Microbiology,* **11**, 35–46 (2003). https://doi.org/10.1111/j.1745-4581.2003.tb00406.x

74. Klungness, L. M., & Peng, Y. S. A histochemical study of pollen digestion in the alimentary canal of honeybees (*Apis mellifera L.*). *Journal of Insect Physiology*, **30**, 511-521. (1984). https://doi.org/10.1016/0022-1910(84)90077-5

75. Khan, K. A., Al-Ghamdi, A. A., Ghramh, H. A., & Hafeez, M. (2020). Structural diversity and functional variability of gut microbial communities associated with honey bees. *Microbial pathogenesis*, **138**, 103793 (2020). https://doi.org/10.1016/j.micpath.2019.103793

76. Zourob, M., Elwary, S., & Turner, A. P. (Eds.). Principles of bacterial detection: biosensors, recognition receptors and microsystems. (Springer Science & Business Media.Receptors, 2008)

77. Stevens, K. A., & Jaykus, L. A. Bacterial separation and concentration from complex sample matrices: a review. *Critical reviews in microbiology*, **30**, 7-24 (2004). https://doi.org/10.1080/10408410490266410

78. Molloy, P., Brydon, L., Porter, A. J., & Harris, W. J. Separation and concentration of bacteria with immobilized antibody fragments. *Journal of applied bacteriology*, **78**, 359-365 (1995). https://doi.org/10.1111/j.1365-2672.1995.tb03418.x

79. Ji, Z., Pinon, D. I., & Miller, L. J. Development of magnetic beads for rapid and efficient metal-chelate affinity purifications. *Analytical biochemistry*, **240**, 197-201 (1996). https://doi.org/10.1006/abio.1996.0349

80. Dryden, S. C., Nahhas, F. A., Nowak, & Tainsky, M. A. Role for human SIRT2 NAD-dependent deacetylase activity in control of mitotic exit in the cell cycle. *Molecular and cellular biology*, **23**, 3173-3185 (2003). DOI: 10.1128/MCB.23.9.3173-3185.2003

81. Ohtsuki, T., Sakurai, M., Sato, A., & Watanabe, K. Characterization of the interaction between the nucleotide exchange factor EF-Ts from nematode mitochondria and elongation factor Tu. *Nucleic acids research*, **30**, 5444-5451 (2002). https://doi.org/10.1093/nar/gkf679

82. Cargile, B. J., Bundy, J. L., Freeman, T. W., & Stephenson, J. L. Gel based isoelectric focusing of peptides and the utility of isoelectric point in protein identification. *Journal of proteome research*, **3**, 112-119 (2004). https://doi.org/10.1021/pr0340431

83. Karam, L., Jama, C., Dhulster, P., & Chihib, N. E. Study of surface interactions between peptides, materials and bacteria for setting up antimicrobial surfaces and active food packaging. J. Mater. *Environ. Sci*, **4**, 798-821 (2013).

84. Najjar, A., Sabri, S., Al-Gaashani, R. & Atieh, M. A. Enhanced fouling resistance and antibacterial properties of novel graphene oxide-Arabic gum polyethersulfone membranes. *Applied Sciences*, **9**, 513 (2019). doi:10.3390/app9030513

85. Cruz, C. F., Martins, M., Egipto, J. & Cavaco-Paulo, A. Changing the shape of hair with keratin peptides. *RSC advances*, **7**, 51581-51592 (2017). doi:10.1039/C7RA10461H

86. Ramadan, M. F., & Al-Ghamdi, A. Bioactive compounds and health-promoting properties of royal

jelly: A review. *Journal of functional foods*, **4**, 39-52. (2012).

87. Viuda-Martos, M., Ruiz-Navajas, Y., Fernández-López, J., & Pérez-Álvarez, J. A. Functional properties of honey, propolis, and royal jelly. *Journal of food science*, **73**, 117–124 (2008).

Appendix

Appendix I

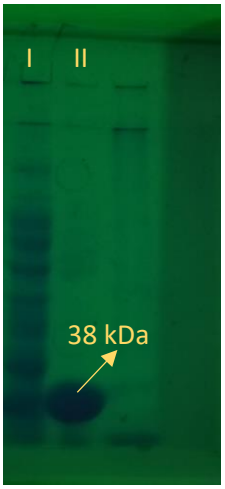

Figure A. 1. SDS-Page electrophoresis of CBD. Identification of CBD, with a single migration band of 38 kDa. Lane I – first fraction of elution with 300 mM imidazole; Lane II – second fraction of elution with 300 mM imidazole.

Appendix II

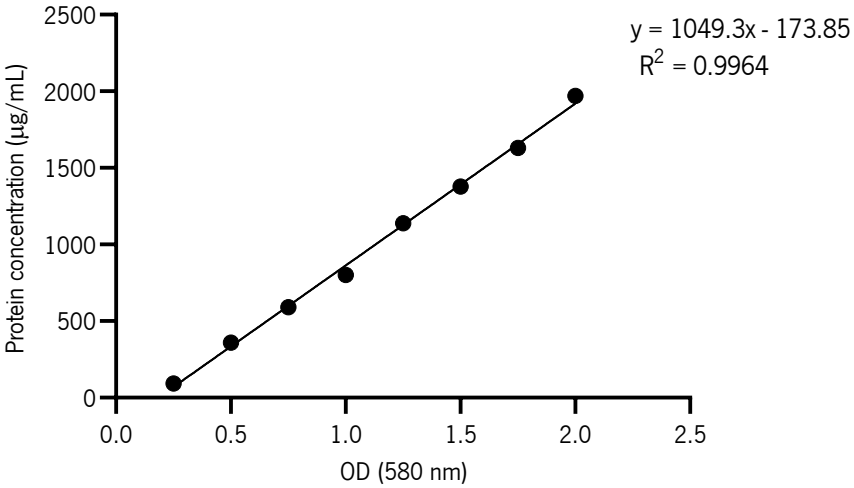

Figure A. 2. Calibration curve Absorbance vs. protein concentration for protein quantification by BCA method.

Appendix III

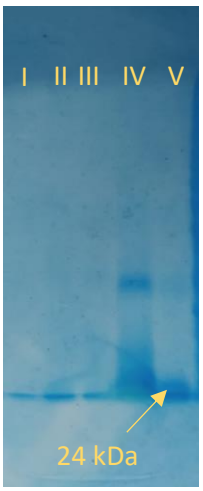

Figure A. 3. SDS-Page electrophoresis of KP-Cryst. Identification of KP-Cryst, with a migration band of ~24 kDa. Lane I – elution with 100 mM imidazole; Lane II – elution with 250 mM imidazole; Lane III – first fraction of elution with 500 mM imidazole; Lane IV – second fraction of elution with 500 mM imidazole; Lane V – third fraction of elution with 500 mM imidazole.

Appendix IV

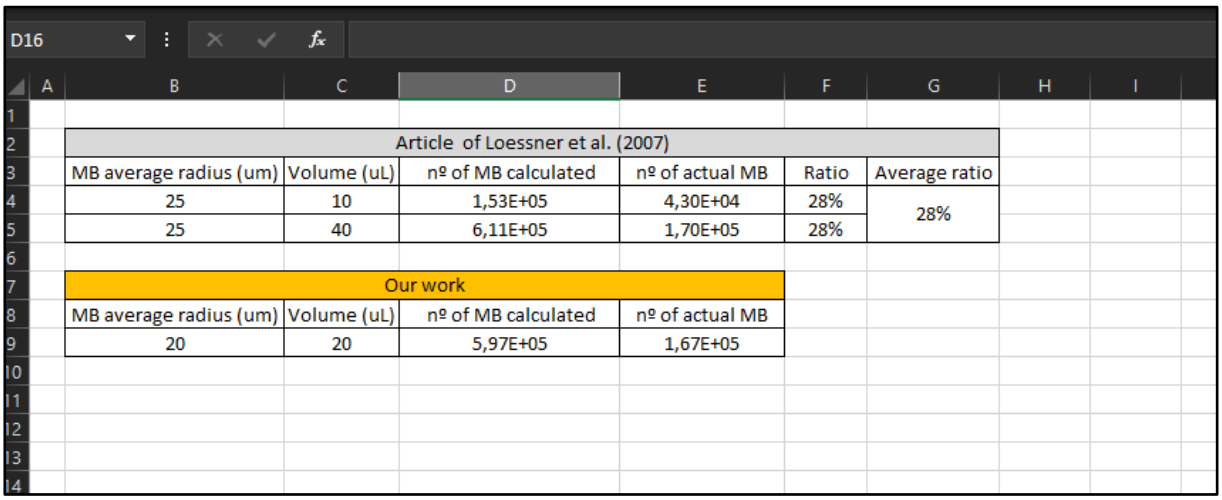

	Article of Loessner et al. (2007)					
	MB average radius (um)	Volume (uL)	nº of MB calculated	nº of actual MB	Ratio	Average ratio
	25	10	1,53E+05	4,30E+04	28%	28%
	25	40	6,11E+05	1,70E+05	28%	

	Our work			
	MB average radius (um)	Volume (uL)	nº of MB calculated	nº of actual MB
	20	20	5,97E+05	1,67E+05

Figure A. 4. Representation of the determination of the number of MB used in our assays, which was an estimate based on the study reported by Loessner et al. (2007), being calculated as follows. Knowing the bead suspension volume and the average MB radius, the division of the sample volume by the volume of a single bead ($4/3\ \pi r^3$), would give us an estimate of beads present in that suspension. According to Loessner and colleagues (2007), beads possess an average radius of 25 µm, therefore, considering our strategy, 40 µl of bead suspension contains 6.11×10^5 beads (number of calculated MB). Nevertheless, through a calibrated microscope grid counting chamber they determinate that the latter volume of bead suspension contains 1.72×10^5 beads (number of actual MB). So, the division of the actual MB calculation by the MB calculated gave us the ratio/percentage (0.28 or 28 %), which we would then use to determinate the number of beads used in our tests, in a closer approximation to reality. Hence, in our study, 20 µl of bead suspension with an average radius of 20 µm, contains 5.97×10^6 beads (number estimated). Multiplying by 0.28, we will have 1.67×10^5 beads (actual number of MB based on the article).

Appendix V

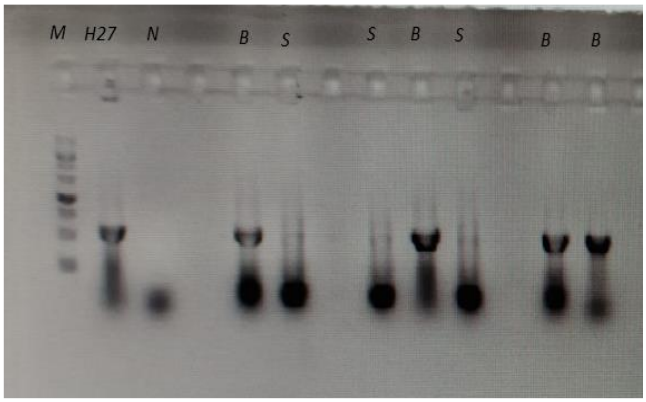

Figure A. 5. Identification of *P. larvae* colonies (derived from spores captured in water by MB-KP-Cryst-Sp system) with a single migration band of 1000 bp. Lane M – Marker; Lane H 27 - PI02-27 vegetative cells, acting as positive control; Lane N – negative control; Lanes B – colonies of *P. larvae;* Lanes S – colonies of unknown microorganism.